Bioorganic Chemistry 109 (2021) 104705

Contents lists available at ScienceDirect

Bioorganic Chemistry

journal homepage: www.elsevier.com/locate/bioorg

# Synthesis, anticancer evaluation and mechanism studies of novel indolequinone derivatives of ursolic acid

Wen-Yan Wang, Wen-Yi Wu, A-Liang Li, Qing-Song Liu, Yue Sun, Wen Gu *

*Jiangsu Provincial Key Lab for the Chemistry and Utilization of Agro-forest Biomass, Jiangsu Key Lab of Biomass-based Green Fuels and Chemicals, Co-Inovation Center for Efficient Processing and Utilization of Forest Products, College of Chemical Engineering, Nanjing Forestry University, Nanjing 210037, PR China*

ARTICLE INFO

*Keywords:*
Ursolic acid
Indolequinone
Anticancer
PI3K/AKT/mTOR signaling pathway
Apoptosis

ABSTRACT

A series of novel indolequinone derivatives of ursolic acid bearing ester, hydrazide, or amide moieties were designed, synthesized, and screened for their *in vitro* antiproliferative activities against three cancer cell lines (MCF-7, HeLa, and HepG2) and a normal gastric mucosal cell line (Ges-1). A number of compounds showed significant activity against tested cancer cell lines. Among them, compound **6t** exhibited the most potent activity against three cancer cell lines with $IC_{50}$ values of 1.66 ± 0.21, 3.16 ± 0.24, and 10.35 ± 1.63 μM, respectively, and considerably lower cytotoxicity to Ges-1 cells. Especially, compound **6t** could arrest cell cycle at S phase, suppress the migration of MCF-7 cells, elevate intracellular reactive oxygen species (ROS) level, and decrease mitochondrial membrane potential. Western blot analysis showed that compound **6t** upregulated Bax, cleaved caspase-3/9, cleaved PARP levels and downregulated Bcl-2 level of MCF-7 cells. All these results indicated that compound **6t** could significantly induce the apoptosis of MCF-7 cells. Meanwhile, compound **6t** markedly decreased p-AKT and p-mTOR expression, which revealed that compound **6t** probably exerted its cytotoxicity through targeting PI3K/AKT/mTOR signaling pathway. Therefore, compound **6t** could be a promising lead for the discovery of novel anticancer agents.

## 1. Introduction

The incidence and mortality of cancer are rapidly growing worldwide, which causes tremendous threat to human life and health. According to Annual World Cancer Report, there were approximately 18.1 million new cases and 9.6 million cancer deaths worldwide in 2018 [1]. Moreover, cancer cases are expected to rise to almost 20 million by 2025 [2]. Despite chemotherapy was considered as one of the most effective methods for cancer treatment in the past few decades, the severe side effects and rapidly occurred drug-resistance have dramatically reduced its clinical efficacy [3,4]. Therefore, there is still an urgent demand in developing new anticancer agents with a better therapeutic index.

Natural products have been considered as a rich source of the basic scaffold for drug discovery. The majority of anticancer drugs currently used are derived from natural product scaffolds [5]. Triterpenoids contains a large number of natural products with diverse structures. In particular, many triterpenes exhibit various biological activities without significant toxicity even at high concentrations [6–8]. Ursolic acid (UA, **1**) is a natural ursane-type triterpenoid abundant in many traditional Chinese medicines. UA and its derivatives have been reported to exhibit a variety of biological activities such as antimicrobial [9], antiviral [10], anti-inflammatory [11], antidiabetic [12], antiulcer [13], anti-osteoporosis [14] and anti-neurodegenerative activities [15]. In addition, many UA derivatives have demonstrated prominent anticancer activities through different mechanisms including regulation of apoptosis, inhibition of DNA polymerase, modulation of signal transductions and interfere with angiogenesis and metastasis [16–18]. Therefore, UA could be a promising starting material for the development of novel anticancer agents.

Heterocycles are considered as privileged scaffolds in drug discovery and widely used in medicinal chemistry [19,20]. Connecting nitrogen-containing heterocyclic structures to certain drug precursors can often enhance biological activity [21]. Concerning the drugs approved by the Food and Drug Administration, 59% of unique small molecule drugs contain nitrogen heterocyclic compounds [22]. Indolequinone is a kind of important heterocycle that is widely present in many drugs or bioactive molecules. Previous studies have shown that indolequinone derivatives have multiple functions such as antibacterial, anti-inflammatory, anti-cancer, and antioxidant properties [23,24]. Some natural products (Fig. 1) bearing indolequinone pharmacophore are

* Corresponding author.
*E-mail address:* njguwen@163.com (W. Gu).

https://doi.org/10.1016/j.bioorg.2021.104705
Received 15 September 2020; Received in revised form 15 December 2020; Accepted 28 January 2021
Available online 9 February 2021
0045-2068/© 2021 Elsevier Inc. All rights reserved.

powerful anticancer agents such as mitomycin C (MMC) [25], murrayaquinone A and B [26], exiguamine A [27], zyzzyanone B [28], and BE-10988 [29]. Inspired by these natural molecules, a large number of synthetic indolequinones have been developed, including the MMC analogue apaziquone (EO9) (Fig. 1), which is currently in advanced clinical trials as a treatment for bladder cancer [30]. Due to their potent biological activities, it is speculated that the fusion of indolequinone moiety with the molecule of UA would probably change its physicochemical properties and lead to better biological activities.

On the other hand, previous studies indicated that the incorporation of polar moiety onto the C-3 or C-28 position of UA might improve its solubility and bioavailability [31,32]. In a former literature, UA was conjugated with different amino acids on the C-28 carboxyl groups. Some derivatives with amino groups exhibited more potent cytotoxic activity than UA and the derivatives bearing carboxyl groups [33]. The hydrazide moiety is also an important pharmacophore in drug development. Many compounds containing hydrazide groups exhibit potent antiviral, anti-inflammatory, and anti-cancer biological activities [34–36]. Therefore, the introduction of amide and hydrazide moieties to the molecule of UA might also produce derivatives with promising anticancer activities. In continuation of our research on novel antitumor derivatives of UA [37,38], we would like to report the synthesis and cytotoxic activities of a new series of indolequinone derivatives of UA. In addition, the preliminary studies on the anticancer mechanisms of representative compound **6t** were also presented.

## 2. Results and discussion

### 2.1. Chemistry

The title derivatives (**6a-t**) were designed and synthesized according to the procedure described in Scheme 1. First, the starting material UA (**1**) was oxidized by Jones reagent to form 3-oxo-ursolic acid (**2**) in 77% yield. Subsequently, the indole derivative **3** was synthesized from compound **2** and 3,5-dimethoxyphenyl hydrazine hydrochloride in 57% yield through Fisher indole reactions. Further, compound **3** was treated with $POCl_3$ and DMF, then hydrolyzed to obtain compound **4** in 74% yield, which was oxidized with $H_2O_2$ to obtain the indolequinone derivative **5** in 71% yield. Concerning the modification of carboxyl group in compound **5**, the carboxyl groups were treated with thionyl chloride to give the 28-acylchloride derivatives, which were then reacted with different alcohols in the presence of $Et_3N$ to afford the corresponding ester products **6a-d** in 80 ~ 89% yields. Further, compounds **5** were reacted with different hydrazides in similar procedure to obtain the acylhydrazine derivatives **6e-j** in 72 ~ 76% yields. On the other hand, compounds **5** were converted to amide derivatives **6k–t** in 67 ~ 78% yields by reacting with the corresponding amine, 1-hydroxybenzotriazole (HOBt) and dicyclohexylcarbodiimide (DCC). All the synthesized title compounds were purified by recrystallization or silica gel column chromatography.

The structures of these compounds were characterized by their HRMS, $^1$H NMR and $^{13}$C NMR spectra. As for a typical example **6t**, its molecular formula was determined to be $C_{43}H_{63}N_3O_4$ through its HRMS spectrum (*m/z* $[M+H]^+$ calcd for $C_{43}H_{64}N_3O_4$: 686.4897; found: 686.4901). IR spectrum of **6t** exhibited broad bands at 3417 and 3223 $cm^{-1}$ corresponding to the N—H stretching of the amide group and indolequinone ring. It also showed strong to medium absorptions around 3000 ~ 2850 $cm^{-1}$ contributing to the C—H stretching of $sp^3$ carbon atoms. Moreover, the strong absorption bands at 1662 and 1641 $cm^{-1}$ were due to the C═O stretching vibrations of amide group and quinone ketones. In its $^1$H NMR spectrum, five singlets at $\delta$ 0.84, 0.91, 1.11, 1.20 and 1.28 ppm could be assigned to five methyl groups at C23 ~ C27, while the doublet at $\delta$ 0.89 ppm and the broad singlet at $\delta$ 0.95 ppm were due to the two adjacent methyl groups at C29 and C30. Concerning the amide side chain, the singlet with six protons at $\delta$ 2.30 ppm could be attributed to the two methyl groups at C7′ and C8′. The multiplets at $\delta$ 3.04 and 3.35 ppm were due to the methylene protons at *C*2′, while the multiplet at $\delta$ 2.40 ppm could be assigned to the methylene at C5′. The singlet at $\delta$ 3.81 ppm could be attributed to the methoxyl group connected to the quinone moiety. The two singlets at $\delta$ 5.39 and 5.65 ppm were the signals of the olefinic hydrogen at C12 and the aromatic proton at C35, respectively. In addition, the triplet at $\delta$ 6.12 ppm and the broad singlet at $\delta$ 9.51 ppm could be assigned to N—H signals in the amide group and indolequinone moiety, respectively. In the $^{13}$C NMR spectrum of **6t**, there were 42 peaks appearing in the range of $\delta$ 10 ~ 185 ppm corresponding to 43 carbon atoms. Specifically, eight peaks at $\delta$ 100 ~ 160 ppm were due to two olefinic carbons at C12 and C13, and six aromatic carbons in the indolequinone moiety. Among them, The peaks at $\delta$ 160.16 and 107.09 ppm could be assigned to C34 and its adjacent carbon (C35), respectively. In addition, the peaks at $\delta$ 170.40 and 185.09 ppm were the signals of two carbonyl groups in the quinone ring (C33 and C36, respectively), while the signal at $\delta$ 178.14 ppm could be attributed to the amide carbonyl group (C28). In the range $\delta$ 10 ~ 60 ppm, the peak at $\delta$ 44.89 ppm (2C) could be assigned to the two methyl groups at C7′ and C8′. The assignments of the signals in the $^1$H and $^{13}$C NMR spectra of compound **6t** were in good accordance with its structure.

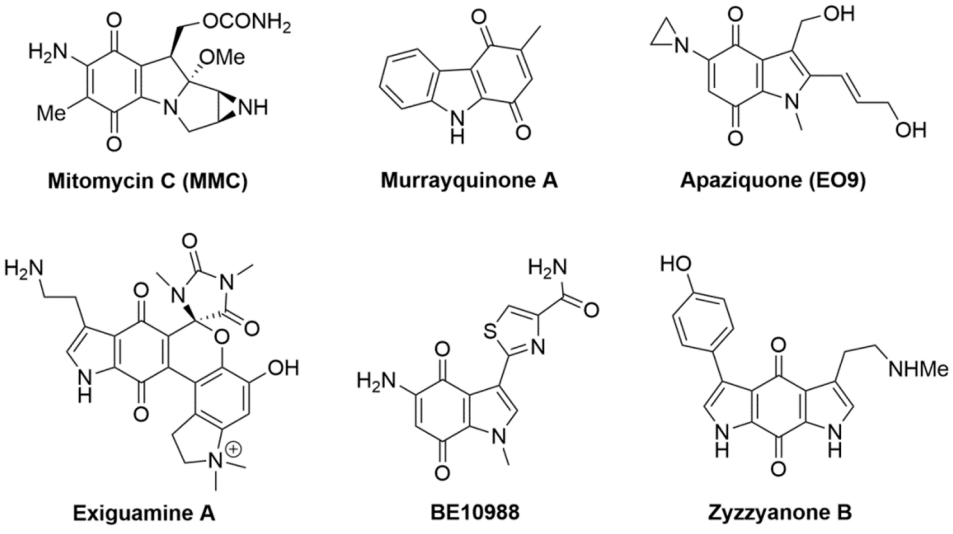


**Fig. 1.** Representative indolequinone derivatives with antitumor activities.

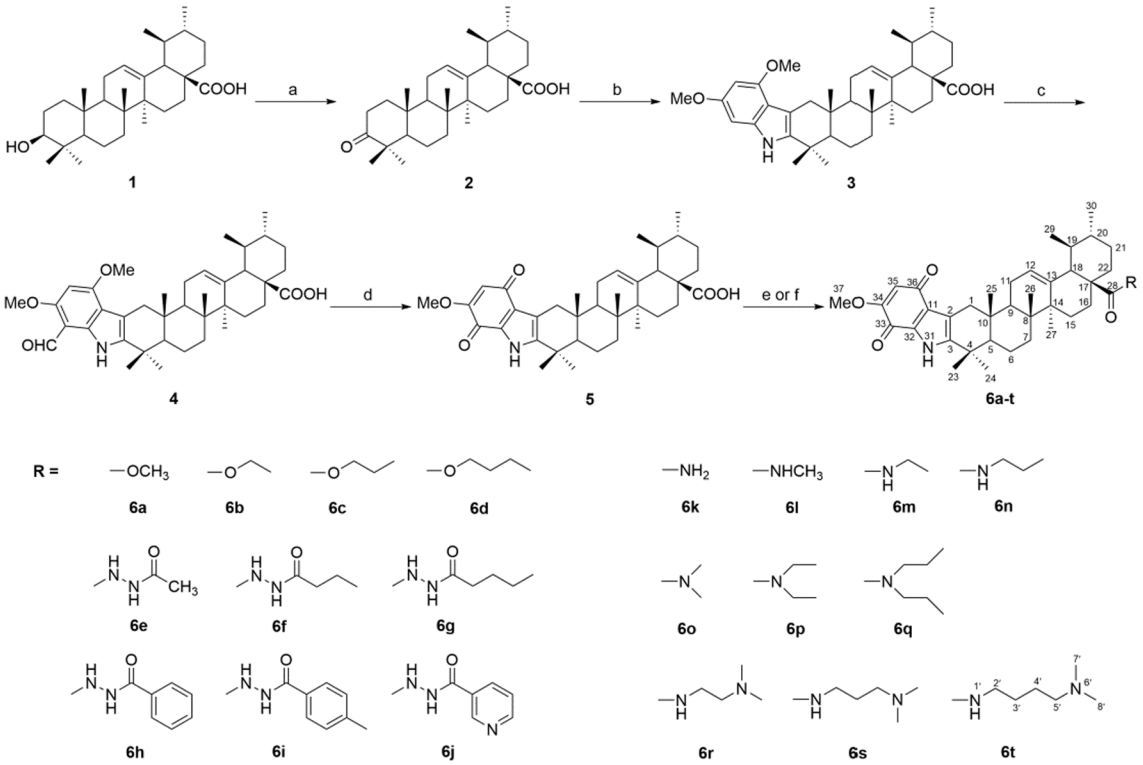


**Scheme 1.** Synthesis of the title indolequinone derivatives. Reagents and experimental conditions were as follows: (a) Jones reagent, acetone, 0 °C, 5 h; (b) (3,5-dimethoxyphenyl)hydrazine, EtOH, conc. HCl, reflux for 4 h; (c) $POCl_3$, DMF, rt, 3 h. (d) $H_2O_2$, HCl, MeOH, 0 °C, 3 h; (e) i. $SOCl_2$, benzene, reflux for 3 h; ii. ROH or $RCONHNH_2$, $Et_3N$, $CH_2Cl_2$/ether, rt, 8 ~ 12 h for compounds **6a-j**; (f) the corresponding amine, HOBt, DCC, $CH_2Cl_2$, rt, 12 h, for compounds **6 k-t**.

### 2.2. Cytotoxic assay

The *in vitro* cytotoxic activity of the title compounds were evaluated by MTT assay against human breast cancer cell line (MCF-7), cervical carcinoma cell line (HeLa), hepatocarcinoma cell line (HepG2) and human normal gastric mucosal cell line (Ges-1). Etoposide was co-assayed as the positive control. All tested compounds were dissolved in DMSO and the stock solutions were diluted by DMEM medium before treatment of the cultured cells. The $IC_{50}$ values of the tested compounds against three cell lines were shown in Table 1.

Among ester derivatives **6a-d**, compounds **6b-d** exhibited strong cytotoxic activities against MCF-7 and HeLa cells at low μM levels ($IC_{50}$ < 5 μM) and moderate activities against HepG2 cells. As for acylhydrazine derivatives **6e-j**, most compounds showed moderate activities against MCF-7 cells and HeLa cells, while they were almost inactive to HepG2 cells lines ($IC_{50}$ > 50 μM). Regarding amide derivative **6 k-t**, compounds **6 k-q** generally displayed considerable activities against MCF-7 cells and relatively weaker activities against HeLa cells, while they only showed mild or no cytotoxicity against HepG2 cell lines. Compounds **6r-t** with dimethylamino group on amide side chain showed potent cytotoxicity against MCF-7 and HeLa cells ($IC_{50}$ < 5 μM). It is worth noting that compound **6t** exhibited the most potent cytotoxic activity against MCF-7 and HeLa cells with $IC_{50}$ values of 1.66 ± 0.21 and 3.16 ± 0.24 μM, respectively, stronger than positive control etoposide. Especially, the compound showed substantially lower cytotoxicity against Ges-1 cells ($IC_{50}$: 20.74 ± 0.61 μM), indicating good selectivity of cytotoxicity (12.5) to MCF-7 and Ges-1 cells, which was also better than that of etoposide (4.0) (Fig. 2). Hence, compound **6t** was selected for further investigations on its anticancer mechanisms.

From above-mentioned results, some preliminary structure–activity relationships (SAR) could also be deduced. Most title derivatives bearing the indolequinone heterocycles exhibited substantially stronger cytotoxic activity than compound **1**, indicating that the introduction of indolequinone moiety will improve the cytotoxicity of UA derivatives.

**Table 1**
Antiproliferative activities of compounds **1**, **5** and **6a-t**.

| Compd | $IC_{50}$ value (μM) | | | |
|---|---|---|---|---|
| | MCF-7 | HeLa | HepG2 | Ges-1 |
| **1** | >50 | >50 | >50 | NT[a] |
| **5** | 18.03 ± 1.38 | 23.72 ± 3.69 | 21.54 ± 2.12 | >50 |
| **6a** | 11.65 ± 1.21 | 19.33 ± 1.61 | >50 | >50 |
| **6b** | 3.19 ± 0.27 | 3.39 ± 0.34 | 18.50 ± 1.23 | 22.43 ± 0.31 |
| **6c** | 3.31 ± 0.26 | 4.25 ± 0.07 | 14.26 ± 1.31 | 23.17 ± 0.66 |
| **6d** | 3.39 ± 0.72 | 4.23 ± 0.46 | 22.18 ± 1.01 | 23.69 ± 0.54 |
| **6e** | 9.64 ± 0.63 | 13.15 ± 1.93 | 40.65 ± 2.37 | >50 |
| **6f** | 10.79 ± 0.72 | 11.08 ± 0.64 | >50 | NT |
| **6g** | 18.32 ± 0.20 | 26.47 ± 1.53 | >50 | NT |
| **6h** | 37.70 ± 0.82 | 21.56 ± 2.82 | >50 | NT |
| **6i** | 11.70 ± 1.22 | 12.12 ± 1.92 | >50 | NT |
| **6j** | 22.78 ± 1.32 | 16.28 ± 0.59 | >50 | NT |
| **6k** | 18.39 ± 1.97 | 22.46 ± 1.22 | >50 | NT |
| **6l** | 11.84 ± 0.06 | 10.85 ± 0.62 | >50 | NT |
| **6m** | 6.13 ± 0.24 | 14.89 ± 0.83 | 42.16 ± 1.78 | >50 |
| **6n** | 9.04 ± 1.21 | >50 | >50 | >50 |
| **6o** | 30.15 ± 0.17 | 31.17 ± 1.37 | 35.09 ± 1.23 | NT |
| **6p** | 18.76 ± 1.22 | >50 | >50 | NT |
| **6q** | 15.00 ± 1.12 | 33.89 ± 0.72 | 30.38 ± 1.83 | NT |
| **6r** | 2.52 ± 0.07 | 3.47 ± 0.16 | 21.27 ± 2.01 | 21.63 ± 0.27 |
| **6s** | 2.23 ± 0.19 | 3.38 ± 0.60 | 14.90 ± 1.79 | 20.89 ± 0.45 |
| **6t** | 1.66 ± 0.21 | 3.16 ± 0.24 | 10.35 ± 1.63 | 20.74 ± 0.61 |
| Etoposide | 5.14 ± 0.32 | 5.74 ± 0.42 | 8.73 ± 1.21 | 20.71 ± 0.49 |

[a] NT: Not tested.

The substituents derived from the carboxyl group of UA also markedly affected the cytotoxic potencies. Generally, compounds **6a-d** with ester groups showed substantially stronger cytotoxicity to three cancer cell lines than compound **5** with carboxyl group, compounds **6e-j** with acylhydrazine moieties and compounds **6k-q** with amide moieties. Among amide derivatives, compounds **6o-q** showed considerably weaker cytotoxicity, which suggested that the introduction of *N*,*N*-

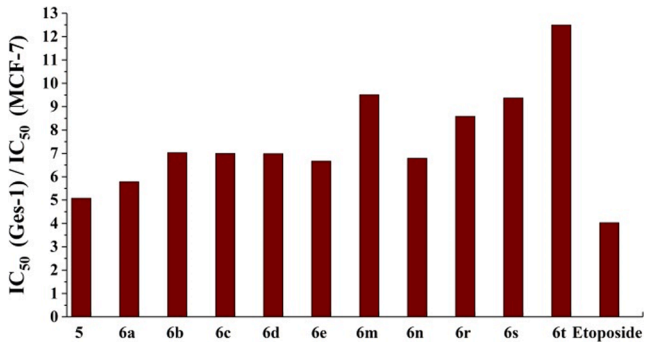


**Fig. 2.** The selectivity of cytotoxicity for some active compounds to MCF-7 and Ges-1 cells.

dialkylamide group will decrease the activity. On the contrary, compounds **6r-t** with dimethylamino groups on the amide side chain displayed much stronger cytotoxic activities than all of the other derivatives, indicating that such moieties on the amide side chain were beneficial to their cytotoxic activity. These preliminary SAR analyses could give useful prompt for the further research on this class of UA derivatives.

### 2.3. Compound **6t** induced cell cycle arrest in MCF-7 cells

To further investigate the antitumor mechanism of action, cell cycle distribution in MCF-7 cells was examined to determine whether or not compound **6t** inhibited the proliferation of cancer cells through cell cycle arrest. MCF-7 cells were treated with different concentrations of compound **6t** (0, 1, 2 and 4 μM) for 48 h. Cell cycle distribution was investigated by flow cytometric analysis after staining the DNA of the treated cells by PI. Cell cycle analysis suggested that treatment of compound **6t** concentration-dependently decreased the population of cells in G0/G1 phase. This phenomenon was accompanied by an increase in the population of cells in S phase. As shown in Fig. 3, the population of MCF-7 cells in the G0/G1 phase decreased from 51.80% (control group) to 36.82% (4 μM group), while the percentage of cells in the S phase increased from 20.85% (control group) to 36.22% (4 μM group). These data indicated that compound **6t** could arrest the cell cycle of MCF-7 cells at the S phase.

### 2.4. Compound **6t** inhibited cell migration of MCF-7 cells

Metastasis is a multistep process involving cancer cell motility and invasion which represents a key difficulty for cancer therapy. Thus, the inhibition of metastasis is vital for efficient cancer treatment. Therefore, the effect of compound **6t** on the migration of cancer cells was investigated by the wound healing assay. As shown in Fig. 4, there was almost complete healing of wound in control group after 48 h, which indicated the considerable migration of cancer cells. However, in 1 μM group, the migration was significantly suppressed compared with the control group. In 2 μM group, the wound was only slightly healed after 48 h, while in 4 μM group, wound healing could not be observed even after 48 h. The results indicated that compound **6t** could markedly suppress the migration of MCF-7 cells in a concentration-dependent manner.

### 2.5. Compound **6t** induced apoptosis of MCF-7 cells

In order to evaluate whether compound **6t** could induce the apoptosis of cancer cells, the Annexin V-FITC/propidium iodide (PI) dual staining assay on MCF-7 cells treated with compound **6t** was carried out through flow cytometry. As shown in Fig. 5, the percentage of early and late apoptotic cells (early apoptosis: Lower right quadrant, AV + / PI—; late apoptosis: Upper right quadrant, AV + /PI + ) significantly increased from 3.24 (0 μM) to 13.22% (1 μM), 27.18 (2 μM) and 34.74% (4 μM), respectively, after treating with different concentrations of **6t** (0, 1, 2 and 4 μM) for 48 h. These results indicated that compound **6t** could trigger the apoptosis of MCF-7 cells in a concentration-dependent manner.

### 2.6. Compound **6t** induced the generation of intracellular ROS

Sufficient evidence revealed that apoptosis induction of cancer cells could be mediated by reactive oxygen species (ROS) in many cellular systems [39]. As a kind of metabolic by products of aerobic respiration, ROS can exert oxidative stress to cells and result in severe damage to organelles [40]. To determine whether the apoptosis was induced by the title compounds, the intracellular ROS level in compound **6t**-treated MCF-7 cells was also examined by using 2′,7′-dichlorodihydrofluorescein diacetate (DCFH-DA), which could be converted into a green fluorescent DCF by ROS oxidation [41]. The MCF-7 cells were treated with different concentrations of compound **6t** for 48 h, and the intracellular fluorescence intensity was quantitatively analysed by flow cytometry. As shown in Fig. 6, upon treatment with different

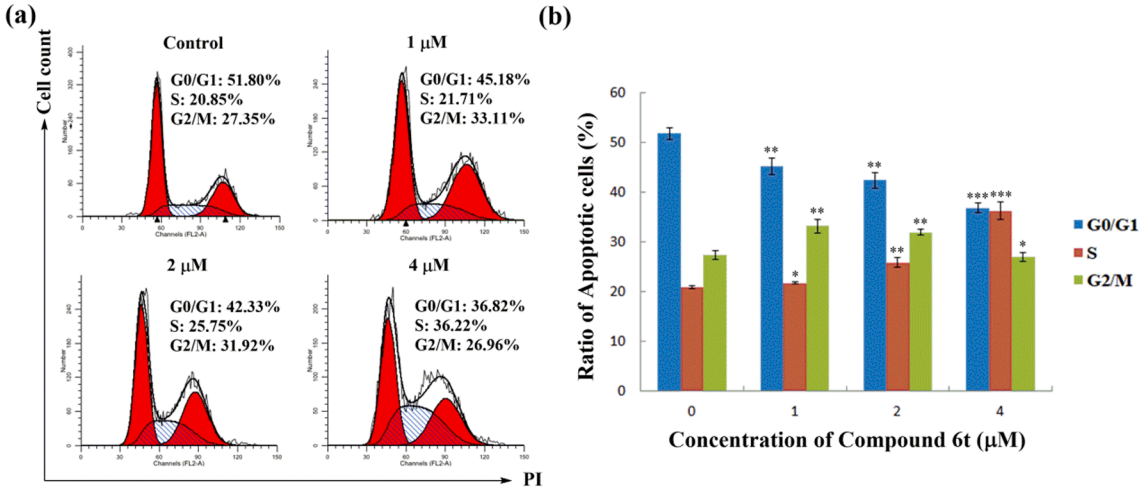


**Fig. 3.** Cell cycle distribution of MCF-7 cells. (a) MCF-7 cells were treated with 0, 1, 2 and 4 μM of compound **6t** for 48 h, stained with propidium iodide (PI) and analyzed for cell cycle by flow cytometry. (b) The column diagram for the cell cycle distribution of MCF-7 cells. *, $p < 0.05$; **, $p < 0.01$; ***, $p < 0.001$ vs. control group.

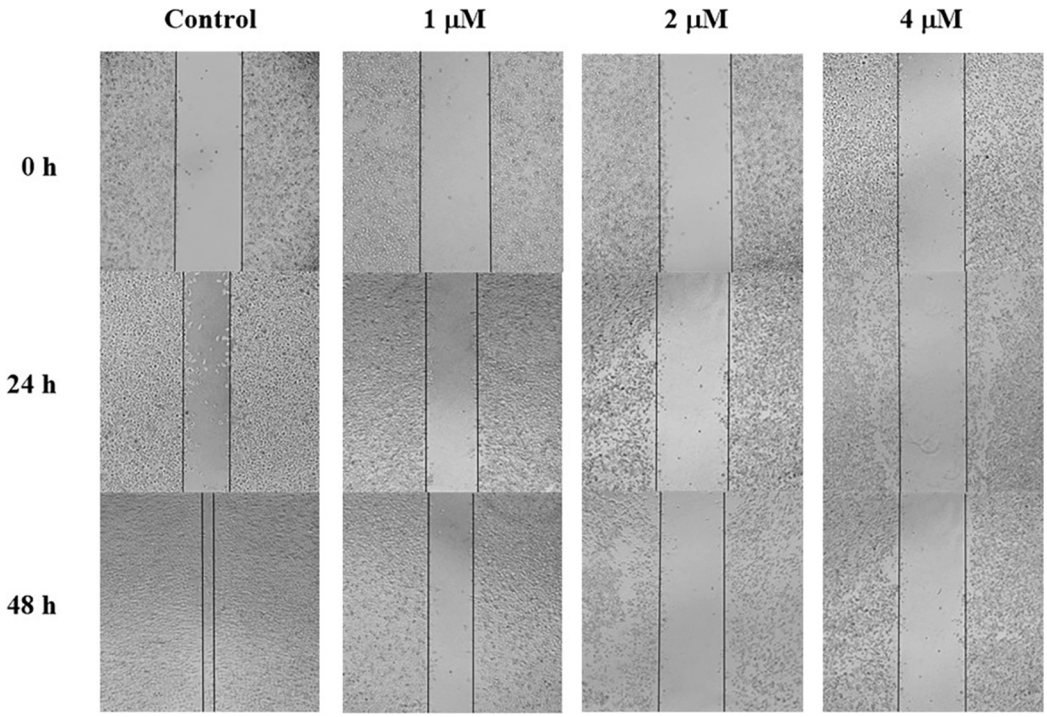


**Fig. 4.** Effect of compound **6t** on *in vitro* migration potential of MCF-7 cells. Scratches were created with sterile 200 μL pipette and images were captured using phase contrast microscopy at 0, 24 and 48 h after treatment with 0, 1, 2 and 4 μM of compound **6t**.

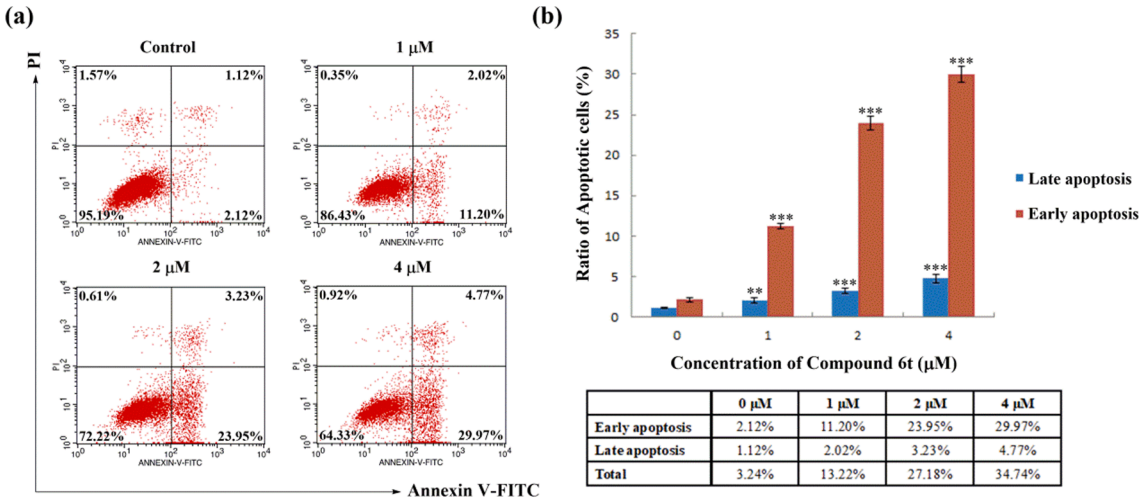


| | 0 μM | 1 μM | 2 μM | 4 μM |
|---|---|---|---|---|
| Early apoptosis | 2.12% | 11.20% | 23.95% | 29.97% |
| Late apoptosis | 1.12% | 2.02% | 3.23% | 4.77% |
| Total | 3.24% | 13.22% | 27.18% | 34.74% |

**Fig. 5.** Annexin V-FITC/PI dual staining assay. (a) MCF-7 cells were treated with compounds **6t** (0, 1, 2 and 4 μM) for 48 h, stained with Annexin V-FITC/PI and analyzed by flow cytometry. (b) The bar diagram for the percentage of early and late apoptotic cells. **, $p < 0.01$; ***, $p < 0.001$ vs. control group.

concentrations of compound **6t**, the percentage of cells with elevated ROS level increased from 3.99% (Control) to 43.23% (4 μM). These results demonstrated that compound **6t** could induce a significant increase of ROS generation in MCF-7 cells in a dose-dependent manner. The elevated intracellular ROS levels indicated that cell apoptosis was correlated with the disruption of the balance between ROS generation and elimination [42]. Therefore, ROS production was responsible for the apoptosis induced by compound **6t**.

### 2.7. Compound 6t reduced the mitochondrial membrane potential (MMP)

It is known that mitochondria play an important role in regulating cellular functions, and the cell apoptosis cannot be reversed when the mitochondrial transmembrane potential collapsed [43]. Mitochondrial dysfunction is one of the most profound features of apoptosis and involves the process, such as mitochondrial permeability transition or the reduction of mitochondrial membrane potential (MMP, $\Delta\Psi_m$) [44]. In order to determine whether compound **6t**-induced apoptosis was involved in a disruption of mitochondrial membrane integrity, we analyzed the $\Delta\Psi_m$ changes by staining MCF-7 cells with JC-1 and analyzing the cells by flow cytometry.

As shown in Fig. 7, the green fluorescence showing the loss of $\Delta\Psi_m$ (Lower right quadrant) in compound **6t**-treated MCF-7 cells increased from 5.51% (control group) to 15.55% (1 μM group), 20.78% (2 μM group) and 31.19% (4 μM group), which indicated that compound **6t** could cause the decrease of mitochondrial membrane potential in a concentration-dependent manner. Therefore, it could be concluded that elevated ROS level and $\Delta\Psi_m$ loss led to mitochondrial damage, which

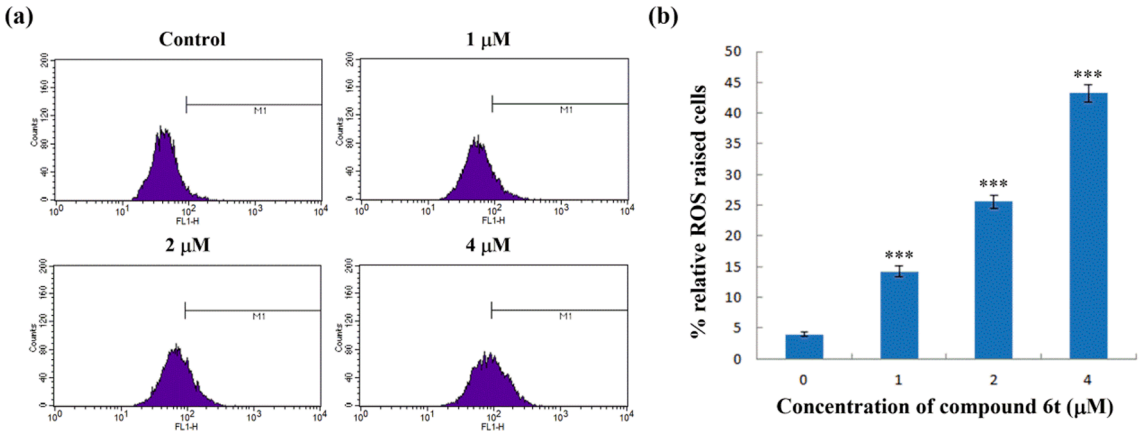


**Fig. 6.** ROS generation of MCF-7 cells induced by compound **6t**. (a) Effect of compound **6t** on the intracellular ROS level in MCF-7 cells. MCF-7 cells were treated with different concentrations of **6t** (0, 1, 2 and 4 μM) for 48 h, incubated with DCFH-DA and analyzed by flow cytometry. (b) The column diagram for the percentage of relative ROS raised cells. ***, $p < 0.001$ vs. control group.

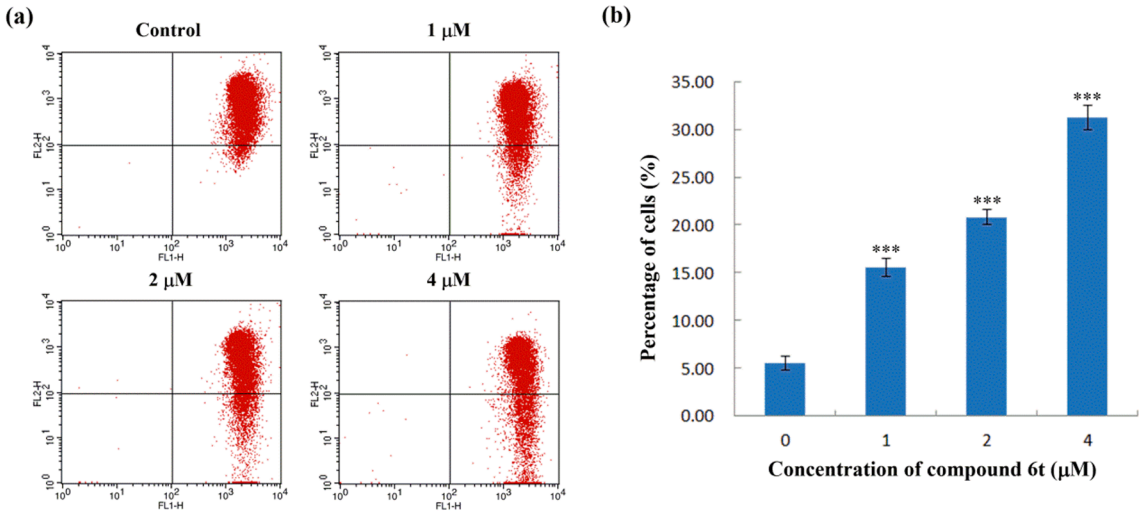


**Fig. 7.** (a) Effect of compound **6t** on mitochondrial membrane potential ($\Delta\Psi_m$). MCF-7 cells were treated with compound **6t** in 0, 1, 2 and 4 μM for 48 h, incubated with JC-1 and analyzed by flow cytometry. (b) The bar diagram for the percentage of cells with low $\Delta\Psi_m$ (Green fluorescence). ***, $p < 0.001$ vs. control group. (For interpretation of the references to colour in this figure legend, the reader is referred to the web version of this article.)

was an important factor responsible for compound **6t**-induced apoptosis.

### 2.8. Compound *6t* regulated the expression of apoptosis-related proteins

To further explore whether compound **6t** induces apoptosis through the mitochondrial signaling pathway, several key protein markers involved in mitochondria-mediated apoptosis were examined by Western blot analysis. Bcl-2 family proteins, mainly including Bax (pro-apoptosis protein) and Bcl-2 (anti-apoptosis protein), are key regulators of mitochondrial integrity [45]. The ratio of Bax/Bcl-2 is vital to determine whether cells will undergo apoptosis. As shown in Fig. 8, the expression level of Bax was obviously upregulated while that of Bcl-2 was decreased after treatment with compound **6t**. Therefore, the ratio of Bax/Bcl-2 increased in a dose-dependent manner (Fig. 8b).

In addition, the collapse of MMP leads to the release of cytochrome *c* from mitochondria to cytosol, which will activate the caspase cascade pathway [46]. Therefore, the expression of cleaved caspase-3 and cleaved caspase-9 were also examined. As shown in Fig. 8c and d, the expression levels of cleaved caspase-3 and cleaved caspase-9 were increased in a concentration-dependent manner. Moreover, poly ADP-ribose polymerase (PARP) plays an essential role in DNA damage repair and maintenance of genomic stability [47]. PARP is the substrate of caspases which cleaves and deactivates PARP during the process of apoptosis [48]. Thus the cleavage of PARP is also a hallmark of apoptosis. As shown in Fig. 8e, the expression level of cleaved PARP was dose-dependently elevated as well. All these results indicated that compound **6t** could induce the apoptosis of MCF-7 cells through the ROS-mediated intrinsic mitochondrial pathway.

### 2.9. Inhibitory effect of compound *6t* on the PI3K/AKT/mTOR signaling pathways

PI3K/AKT/mTOR signaling pathway plays an important role in occurrence and progression of tumor and drug resistance by inducing survival, proliferation, differentiation and vascularization of cancer cells. Thus, this signaling pathway has become an attractive target for cancer treatment [49,50]. Previous literatures demonstrated that ursolic acid displayed anticancer activity by inhibiting the PI3K/AKT/mTOR signaling pathway [51,52]. Therefore, the effects of compound **6t** on the PI3K/AKT/mTOR signaling pathway were explored by Western blot analysis. As shown in Fig. 9, the treatment with compound **6t** down-regulated the levels of phosphorylated-AKT (p-AKT) and phosphorylated-mTOR (p-mTOR) in MCF-7 cells in a concentration-dependent manner, which are key proteins inducing cell proliferation

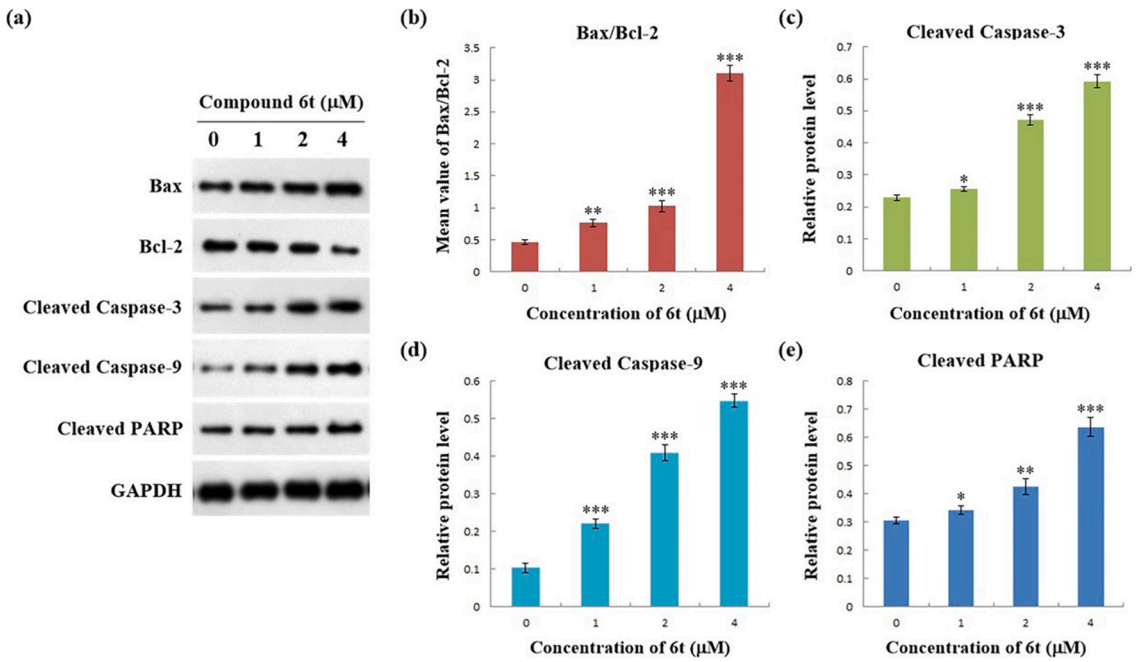


**Fig. 8.** (a) Western blot analysis of the level of Cleaved PARP, Bax, Bcl-2, Cleaved Caspase-3 and Cleaved Caspase-9 in MCF-7 cells treated with compound **6t** (0, 1, 2 and 4 μM) for 48 h. (b) The rate changes of Bax/Bcl-2 in MCF-7 cells. (c) The expression level of Cleaved Caspase-3 in MCF-7 cells. (d) The expression level of Cleaved Caspase-9 in MCF-7 cells. (e) The expression level of Cleaved PARP in MCF-7 cells. *, $p < 0.05$; **, $p < 0.01$; ***, $p < 0.001$ vs. control group.

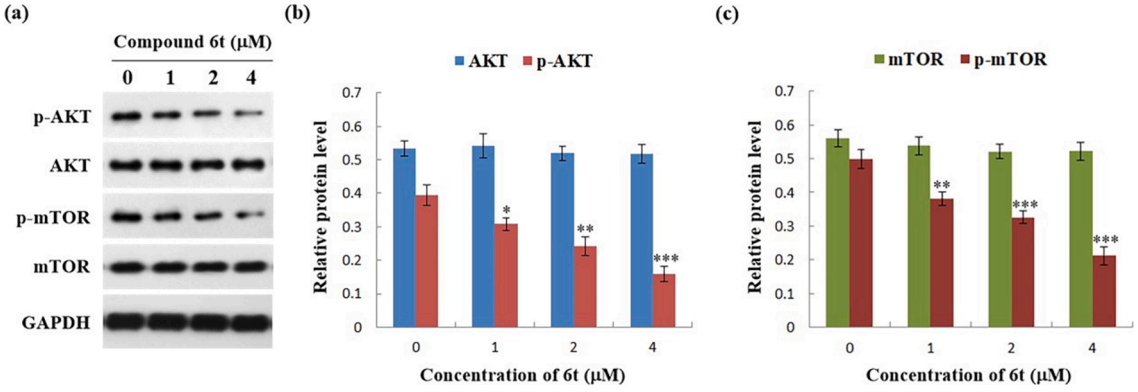


**Fig. 9.** Effect of compound **6t** on PI3K/AKT/mTOR signaling pathway through Western blot analysis. (a) The levels of p-AKT, AKT, p-mTOR and mTOR in MCF-7 cells treated with compound **6t** (0, 1, 2 and 4 μM) for 48 h. (b) The expression levels of p-AKT and AKT in MCF-7 cells. (c) The expression level of p-mTOR and mTOR in MCF-7 cells. *, $p < 0.05$; **, $p < 0.01$; ***, $p < 0.001$ vs. control group.

and apoptosis inhibition in this pathway. The results indicated that compound **6t** probably caused the apoptosis of MCF-7 cells by inhibiting the PI3K/AKT/mTOR signaling pathway.

### *2.10. Cytotoxic mechanisms of compound **6t** on noncancerous Ges-1 cells*

To explore if compound **6t** could inhibit the growth of noncancerous Ges-1 cells through the above-mentioned mechanisms, similar western blot analyses were also carried out on compound **6t**-treated Ges-1 cells. As shown in Fig. 10, the ratio of Bax/Bcl-2 and the expression level of cleaved caspase-3 were increased concentration-dependently, while the expression levels of p-AKT and p-mTOR were decreased in a dose-dependent manner. These results indicated that compound **6t** could inhibit the PI3K/AKT/mTOR signaling pathway and induce the apoptosis of Ges-1 cells, which could be the possible cytotoxic mechanisms of compound **6t** to Ges-1 cells.

## 3. Conclusions

In present study, a series of novel indolequinone derivatives of ursolic acid were designed, synthesised, and evaluated for their *in vitro* antiproliferative activities against three human cancer cell lines (MCF-7, HeLa, and HepG2) and a normal gastric mucosal cell line (Ges-1). As a result, some indolequinone derivatives containing *N*-(dimethylamino) alkyl amide moiety exhibited considerable antiproliferative activity. Among them, compound **6t** showed the most potent inhibitory activity against three cancer cell lines, with $IC_{50}$ values equivalent to or better than those of positive control etoposide. More importantly, compound **6t** displayed substantially lower cytotoxicity to Ges-1 cells. In addition, compound **6t** could arresting cell cycle of MCF-7 cells at the S phase, suppress the migration of MCF-7 cells, enhance the intracellular ROS level, decrease the mitochondrial membrane potential, up-regulate Bax, cleaved caspase-3, cleaved caspase-9 and cleaved PARP levels, reduce Bcl-2 level in a dose-dependent manner, and induce the apoptosis of MCF-7 cells. Western blot analysis also indicated that compound **6t**

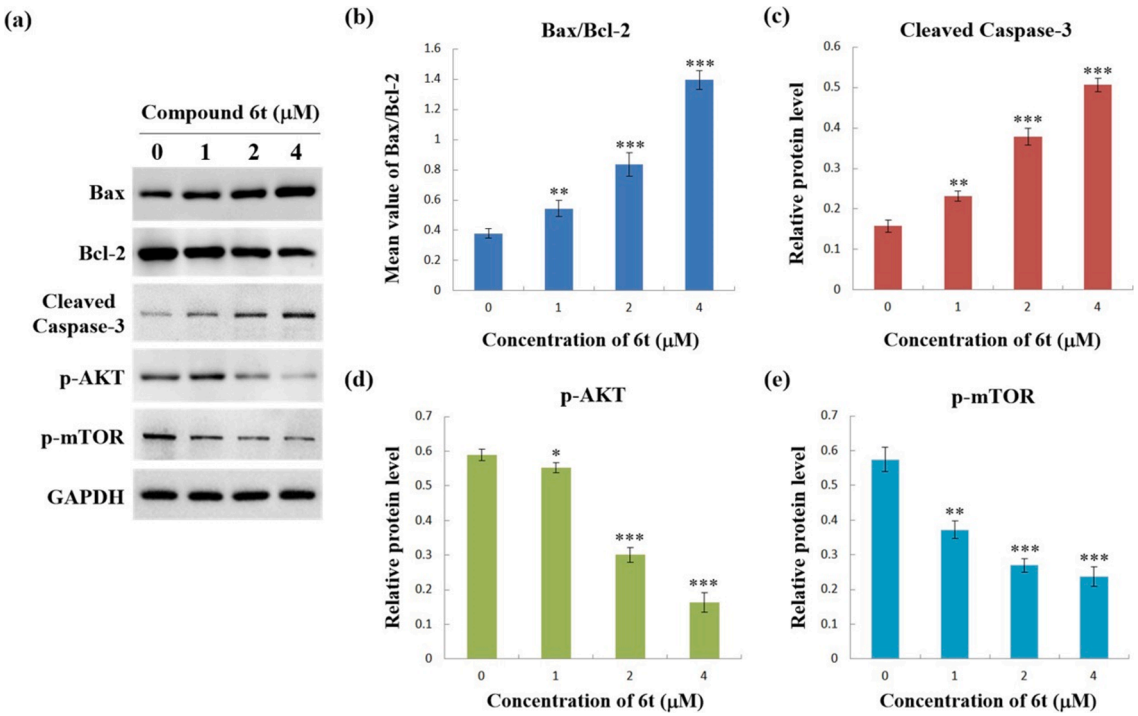


**Fig. 10.** (a) Western blot analysis of the level of Bax, Bcl-2, Cleaved Caspase-3, p-AKT and p-mTOR in Ges-1 cells treated with compound **6t** (0, 1, 2 and 4 μM) for 48 h. (b) The rate changes of Bax/Bcl-2 in Ges-1 cells. (c) The expression level of Cleaved Caspase-3 in Ges-1 cells. (d) The expression level of p-AKT in Ges-1 cells. (e) The expression level of p-mTOR in Ges-1 cells. *, $p < 0.05$; **, $p < 0.01$; ***, $p < 0.001$ vs. control group.

markedly decreased the expression levels of p-AKT and p-mTOR, which revealed that compound **6t** displayed anticancer activity via interfering with PI3K/AKT/mTOR signaling pathway. All these results demonstrate the potential of this compound as promising candidate for the discovery of novel anticancer agents. Other related pathways and protein targets presumably involved in the anticancer effect of this series of UA derivatives will be investigated in future investigations.

## 4. Experimental

### 4.1. General

Melting points were measured on an XT-4 apparatus (Taike Corp, Beijing, China) and were uncorrected. The ESI-MS spectra were recorded on a Mariner System 5304 mass spectrometer. $^{1}H$ and $^{13}C$ NMR spectra were obtained in $CDCl_3$ on Bruker AV-400 and DRX-600 NMR spectrometers (Billerica, MA, USA) using TMS as internal standard. Reactions and the resulted products were monitored by TLC which was carried out on TLC Silica gel 60 $F_{254}$ Aluminium sheets from Merck KGaA, Darmstadt, Germany and visualised in UV light (254 nm). Silica gel (300 ~ 400 mesh) for column chromatography was purchased from Qingdao Marine Chemical Factory, China. The reagents (chemicals), all being of A.R. grade, were purchased from Shanghai Chemical Reagent Company (Shanghai, China) and Energy Chemical (Shanghai, China). UA (95%) was bought from Jingzhu Biological Technology Co, Ltd. (Nanjing, China).

### 4.2. General procedures for the synthesis of compounds *6a-j*.

The key intermediate **5** was synthesized from ursolic acid (**1**) according to the procedure reported before [53], which was further treated as shown in Scheme 1 to afford the title compounds **6a-j**. To the solution of compounds **5** (0.15 mmol) in benzene (5 mL) was added dropwise 200 μL of $SOCl_2$ (1.5 mmol). The reaction mixture was refluxed at 80 °C for 3 h. After cooling, the solvent and excess $SOCl_2$ were removed by concentration *in vacuo*. The corresponding products were dissolved in ether (8 mL) and the mixture of corresponding alcohol or acylhydrazine (0.225 mmol), $Et_3N$ (45 μL), and $CH_2Cl_2$ (2 mL) were slowly added. The reaction mixture was stirred at room temperature for 8–12 h, and monitored by TLC. At the end of reaction, the mixture was poured into 30 mL of ice-cold water and extracted with $CH_2Cl_2$ (3 × 40 mL). The organic layer was combined, washed with water, saturated $NaHCO_3$ and brine, dried over anhydrous $Na_2SO_4$, and concentrated *in vacuo* to obtain a crude product, which was purified by silica gel column chromatography ($CH_2Cl_2$-MeOH 200:1 ~ 50:1, v/v) to afford compounds **6a-j** in 72 ~ 89% yields.

#### 4.2.1. 6′-Methoxy-4′,7′-dioxo-4′,7′-dihydro-1′H-ursa-2,12-dieno[3,2-b] indol-28-oic acid (5)

Red Powder Solid; M.p. 297 ~ 299 °C; Yield: 82%; $^{1}H$ NMR (600 MHz, $CDCl_3$): $\delta$ 0.82 (s, 3H), 0.87 (s, 3H), 0.88 (d, $J$ = 6.5 Hz, 3H), 0.95 (d, $J$ = 6.3 Hz, 3H), 1.10 (s, 3H), 1.15 (m, 1H), 1.19 (s, 3H), 1.30 (m, 1H), 1.33 (s, 3H), 1.29 ~ 2.15 (m, 18H), 2.24 (d, $J$ = 11.2 Hz, 1H), 3.06 (d, $J$ = 16.6 Hz, 1H), 3.80 (s, 3H), 5.32 (brs, 1H), 5.65 (s, 1H), 10.63 (s, 1H); $^{13}C$ NMR (150 MHz, $CDCl_3$): $\delta$ 15.83, 16.87, 16.96, 19.07, 21.16, 23.23, 23.43, 23.45, 24.18, 28.03, 30.59, 30.70, 32.33, 34.22, 36.73, 37.81, 38.03, 38.85, 39.14, 39.53, 42.20, 45.96, 48.05, 52.60, 52.77, 56.57, 107.12, 119.47, 124.57, 125.92, 128.47, 137.70, 147.21, 160.30, 170.50, 182.24, 185.01; IR (KBr, $cm^{-1}$): 3434, 3239, 2926, 2868, 1695, 1644, 1597, 1490, 1451, 1385, 1231, 1115, 1034, 842, 791; HRMS (ESI): $m/z$ $[M+H]^+$ calcd for $C_{37}H_{50}NO_5$: 588.3689; found: 588.3686.

#### 4.2.2. 6′-Methoxy-4′,7′-dioxo-4′,7′-dihydro-1′H-ursa-2,12-dieno[3,2-b] indol-28-oic acid methyl ester (6a)

Red powder solid; M.p. 307 ~ 309 °C; Yield: 82%; $^{1}H$ NMR (400 MHz, $CDCl_3$): $\delta$ 0.81 (s, 3H), 0.88 (d, $J$ = 6.4 Hz, 3H), 0.90 (s, 3H), 0.95 (d, $J$ = 6.1 Hz, 3H), 1.10 (s, 3H), 1.20 (s, 3H), 1.25 (m, 2H), 1.27 (s, 3H), 1.32 (m, 1H), 1.35 ~ 1.75 (m, 11*H*), 1.80 (dd, $J$ = 13.7, 4.4 Hz, 1H), 2.02 (m, 2H), 2.16 (m, 2H), 2.27 (d, $J$ = 11.3 Hz, 1H), 3.07 (d, $J$ = 16.5 Hz, 1H), 3.61 (s, 3H), 3.81 (s, 3H), 5.34 (s, 1H), 5.65 (s, 1H), 9.45 (s, 1H);

$^{13}$C NMR (100 MHz, $CDCl_3$): $\delta$ 15.79, 16.82, 17.00, 19.10, 21.18, 23.43, 23.45, 23.47, 24.29, 28.04, 30.73, 30.88, 32.37, 34.05, 36.63, 37.84, 37.97, 38.88, 39.17, 39.53, 42.22, 45.99, 48.24, 51.49, 52.55, 53.03, 56.54, 107.25, 118.95, 124.24, 125.72, 128.55, 137.87, 146.59, 160.02, 170.56, 178.10, 184.85; IR (KBr, $cm^{-1}$): 3434, 3239, 2926, 2868, 1695, 1644, 1597, 1490, 1451, 1385, 1231, 1115, 1034, 842, 791; HRMS (ESI): *m/z* $[M+H]^+$ calcd for $C_{38}H_{52}NO_5$: 602.3845; found: 602.3840.

#### 4.2.3. 6′-Methoxy-4′,7′-dioxo-4′,7′-dihydro-1′H-ursa-2,12-dieno[3,2-b] indol-28-oic acid ethyl ester (6b)

Red powder solid; M.p. 290 ~ 292 °C; Yield: 89%; $^1$H NMR (400 MHz, $CDCl_3$): $\delta$ 0.83 (s, 3H), 0.88 (d, $J$ = 6.4 Hz, 3H), 0.90 (s, 3H), 0.94 (d, $J$ = 5.8 Hz, 3H), 1.10 (s, 3H), 1.20 (s, 3H), 1.22 (t, $J$ = 7.3 Hz, 3H), 1.25 (m, 2H), 1.28 (s, 3H), 1.29 (m, 1H), 1.33 (m, 2H), 1.40 ~ 1.75 (m, 9H), 1.80 (td, $J$ = 13.7, 4.5 Hz, 1H), 2.02 (m, 2H), 2.14 (m, 2H), 2.28 (d, $J$ = 11.2 Hz, 1H), 3.07 (d, $J$ = 16.5 Hz, 1H), 3.81 (s, 3H, $OCH_3$), 4.07 (q, $J$ = 7.1 Hz, 2H), 5.33 (t, $J$ = 3.6 Hz, 1H), 5.65 (s, 1H), 9.52 (s, 1H); $^{13}$C NMR (100 MHz, $CDCl_3$): $\delta$ 14.26, 15.82, 16.99, 17.02, 19.10, 21.19, 23.36, 23.38, 23.44, 24.25, 28.00, 30.78, 30.87, 32.47, 34.06, 36.66, 37.83, 38.01, 38.88, 39.22, 39.61, 42.29, 46.00, 48.01, 52.57, 53.04, 56.54, 60.04, 107.24, 119.00, 124.26, 125.68, 128.55, 137.88, 145.88, 160.03, 170.55, 177.56, 184.85; IR (KBr, $cm^{-1}$): 3458, 3275, 2925, 2858, 1727, 1667, 1642, 1597, 1494, 1455, 1385, 1231, 1115, 1033, 842, 806; HRMS (ESI): *m/z* $[M+H]^+$ calcd for $C_{39}H_{54}NO_5$: 616.4002; found: 616.3996.

#### 4.2.4. 6′-Methoxy-4′,7′-dioxo-4′,7′-dihydro-1′H-ursa-2,12-dieno[3,2-b] indol-28-oic acid propyl ester (6c)

Red Powder Solid; M.p. 260 ~ 262 °C; Yield: 80%; $^1$H NMR (600 MHz, $CDCl_3$): $\delta$ 0.81 (s, 3H), 0.86 (s, 3H), 0.87 (d, $J$ = 6.5 Hz, 3H), 0.94 (d, $J$ = 6.3 Hz, 3H), 1.09 (s, 3H), 1.14 (d, $J$ = 13.5 Hz, 1H), 1.19 (s, 3H), 1.20 ~ 1.28 (m, 3H), 1.29 (s, 3H), 1.31 ~ 1.45 (m, 5H), 1.50 (m, 2H), 1.56 (s, 1H), 1.57 (s, 1H), 1.65 (dd, $J$ = 13.3, 4.2 Hz, 1H), 1.68 ~ 1.79 (m, 4H), 1.88 (td, $J$ = 13.4, 3.8 Hz, 1H), 2.00 (m, 2H), 2.13 (m, 2H), 2.24 (d, $J$ = 11.3 Hz, 1H), 2.88 (s, 1H), 2.96 (s, 1H), 3.05 (d, $J$ = 16.6 Hz, 1H), 3.80 (s, 3H), 5.29 (s, 1H), 5.31 (t, $J$ = 4.1 Hz, 1H), 5.65 (s, 1H), 10.92 (s, 1H); $^{13}$C NMR (150 MHz, $CDCl_3$) $\delta$ 15.84, 16.87, 16.97, 19.06, 21.19, 23.16, 23.35, 23.42, 24.19, 28.04, 30.54, 30.71, 31.54, 32.33, 34.25, 36.63, 37.79, 38.03, 38.84, 39.13, 39.51, 42.19, 45.94, 48.02, 52.59, 52.76, 53.47, 56.61, 107.09, 119.51, 124.57, 125.88, 128.47, 137.70, 147.40, 160.32, 170.47, 182.92, 185.09; IR (KBr, $cm^{-1}$): 3476, 3232, 2928, 2855, 1737, 1667, 1626, 1597, 1452, 1202, 1107, 1029, 967, 856, 780; HRMS (ESI): *m/z* $[M+H]^+$ calcd for $C_{40}H_{56}NO_5$: 630.4158; found: 630.4149.

#### 4.2.5. 6′-Methoxy-4′,7′-dioxo-4′,7′-dihydro-1′H-ursa-2,12-dieno[3,2-b] indol-28-oic acid butyl ester (6d)

Red powder solid; M.p. 288 ~ 290 °C; Yield: 82%; $^1$H NMR (600 MHz, $CDCl_3$): $\delta$ 0.83 (s, 3H), 0.88 (d, $J$ = 6.7 Hz, 3H), 0.91 (s, 3H), 0.93 (t, $J$ = 7.4 Hz, 3H), 0.95 (d, $J$ = 6.2 Hz, 3H), 1.10 (s, 3H), 1.19 (s, 3H), 1.27 (m, 4H), 1.29 (s, 3H), 1.33 (m, 2H), 1.46 ~ 1.52 (m, 4H), 1.55 ~ 1.75 (m, 8H), 1.81 (td, $J$ = 13.4, 4.3 Hz, 1H), 1.97 ~ 2.05 (m, 2H), 2.15 (m, 2H), 2.28 (d, $J$ = 11.2 Hz, 1H), 3.07 (d, $J$ = 16.5 Hz, 1H), 3.81 (s, 3H), 4.00 (m, 2H), 5.33 (t, $J$ = 3.5 Hz, 1H), 5.65 (s, 1H), 9.28 (s, 1H); $^{13}$C NMR (150 MHz, $CDCl_3$): $\delta$ 13.73, 15.79, 16.97, 17.02, 19.10, 19.26, 21.16, 23.38, 23.42, 23.48, 24.26, 28.00, 30.68, 30.89, 31.61, 32.46, 34.02, 36.71, 37.82, 37.96, 38.88, 39.20, 39.58, 42.27, 45.98, 48.17, 52.54, 53.04, 56.52, 63.98, 107.23, 118.95, 124.23, 125.69, 128.58, 137.90, 145.75, 159.99, 170.54, 177.63, 184.80; IR (KBr, $cm^{-1}$): 3444, 3236, 2926, 2872, 1725, 1666, 1646, 1597, 1491, 1452, 1032, 1230, 1261, 1115, 843, 794; HRMS (ESI): *m/z* $[M+H]^+$ calcd for $C_{41}H_{58}NO_5$: 644.4315; found: 644.4314.

#### 4.2.6. 6′-Methoxy-4′,7′-dioxo-4′,7′-dihydro-1′H-ursa-2,12-dieno[3,2-b] indol-28- (2-acetylhydrazide) (6e)

Red powder solid; M.p. 279 ~ 281 °C; Yield: 72%; $^1$H NMR (600 MHz, $CDCl_3$): $\delta$ 0.79 (s, 3H), 0.88 (d, $J$ = 6.7 Hz, 3H), 0.89 (s, 3H), 0.94 (s, 3H), 1.11 (s, 3H), 1.24 (s, 3H), 1.26 (m, 2H), 1.30 (s, 3H), 1.31 (m, 1H), 1.36 (d, $J$ = 10.6 Hz, 1H), 1.43 ~ 1.60 (m, 7H), 1.66 ~ 1.76 (m, 4H), 1.85 (d, $J$ = 12.7 Hz, 1H), 2.03 (s, 3H), 2.07 (m, 2H), 2.14 (d, $J$ = 16.9 Hz, 1H), 2.19 (m, 1H), 3.06 (d, $J$ = 16.5 Hz, 1H), 3.78 (s, 3H, $OCH_3$), 5.52 (brs, 1H), 5.65 (s, 1H), 9.00 (d, $J$ = 4.7 Hz, 1H), 9.85 (m, 1H), 10.91 (m, 1H); $^{13}$C NMR (150 MHz, $CDCl_3$) $\delta$ 15.91, 16.43, 17.06, 19.04, 20.62, 21.15, 23.04, 23.24, 23.52, 24.84, 27.77, 30.59, 30.79, 32.15, 34.30, 37.11, 37.73, 38.17, 38.85, 39.58, 39.65, 42.49, 45.98, 47.58, 52.65, 53.45, 56.53, 107.12, 119.08, 124.39, 127.21, 128.64, 138.35, 146.85, 160.25, 166.29, 170.57, 173.72, 185.04; IR (KBr, $cm^{-1}$): 3257, 2928, 2870, 1662, 1639, 1596, 1487, 1456, 1385, 1263, 1231, 1115, 1031, 842, 792; HRMS (ESI): *m/z* $[M+H]^+$ calcd for $C_{39}H_{54}N_3O_5$: 644.4063; found: 644.4066.

#### 4.2.7. 6′-Methoxy-4′,7′-dioxo-4′,7′-dihydro-1′H-ursa-2,12-dieno[3,2-b] indol-28-[2-(1- oxobutyl)hydrazide] (6f)

Red powder solid; M.p. 265 ~ 267 °C; Yield: 72%; $^1$H NMR (600 MHz, $CDCl_3$): $\delta$ 0.79 (s, 3H), 0.85 ~ 1.92 (m, 9H), 0.95 (s, 3H), 1.12 (s, 3H), 1.23 (s, 3H), 1.29 (m, 2H), 1.30 (s, 3H), 1.31 (m, 1H), 1.38 (d, $J$ = 10.1 Hz, 1H), 1.44 (m, 2H), 1.50 ~ 1.60 (m, 5H), 1.65 (m, 3H), 1.74 (m, 3H), 1.88 (d, $J$ = 13.1 Hz, 1H), 2.09 (m, 2H), 2.15 (d, $J$ = 17.0 Hz, 1H), 2.20 (m, 1H), 2.23 (t, $J$ = 7.3 Hz, 2H), 3.07 (d, $J$ = 16.5 Hz, 1H), 3.80 (s, 3H, $OCH_3$), 5.57 (brs, 1H), 5.66 (s, 1H), 9.06 (d, $J$ = 6.0 Hz, 1H), 9.49 (m, 1H), 10.47 (m, 1H); $^{13}$C NMR (150 MHz, $CDCl_3$): $\delta$ 14.09, 15.83, 16.32, 17.06, 18.97, 19.04, 21.12, 22.67, 23.27, 23.54, 24.87, 27.79, 30.66, 30.78, 32.14, 34.24, 35.85, 37.04, 37.75, 38.13, 38.89, 39.62, 39.66, 42.51, 46.02, 47.55, 52.90, 53.39, 56.48, 107.18, 118.98, 124.36, 127.35, 128.65, 138.42, 146.45, 160.19, 168.72, 170.59, 173.41, 184.90; IR (KBr, $cm^{-1}$): 3241, 2926, 2854, 1644, 1595, 1489, 1457, 1334, 1231, 1115, 1030, 842, 792; HRMS (ESI): *m/z* $[M+H]^+$ calcd for $C_{41}H_{58}N_3O_5$: 672.4376; found: 672.4380.

#### 4.2.8. 6′-Methoxy-4′,7′-dioxo-4′,7′-dihydro-1′H-ursa-2,12-dieno[3,2-b] indol-28-[2-(1- oxopentyl)hydrazide] (6g)

Red powder solid; M.p. 276 ~ 279 °C; Yield: 76%; $^1$H NMR (600 MHz, $CDCl_3$): $\delta$ 0.78 (s, 3H), 0.87 ~ 0.91 (m, 9H), 0.96 (s, 3H), 1.13 (s, 3H), 1.22 (s, 3H), 1.28 (m, 2H), 1.29 (s, 3H), 1.32 (m, 3H), 1.38 (m, 1H), 1.46 (m, 2H), 1.50 ~ 1.61 (m, 6H), 1.68 (dd, $J$ = 13.5, 3.8 Hz, 2H), 1.75 (m, 3H), 1.91 (d, $J$ = 14.1 Hz, 1H), 2.01 (d, $J$ = 5.9 Hz, 1H), 2.06 (m, 1H), 2.15 (d, $J$ = 16.4 Hz, 1H), 2.21 (m, 1H), 2.24 (t, $J$ = 7.4 Hz, 2H), 3.08 (d, $J$ = 16.4 Hz, 1H), 3.80 (s, 3H), 5.58 (brs, 1H), 5.65 (s, 1H), 9.03 (d, $J$ = 6.8 Hz, 1H), 9.18 (d, $J$ = 6.7 Hz, 1H), 10.19 (s, 1H); $^{13}$C NMR (150 MHz, $CDCl_3$): $\delta$ 13.68, 15.82, 16.27, 17.06, 19.03, 21.12, 22.21, 22.66, 23.23, 23.54, 24.87, 25.61, 27.50, 30.72, 31.91, 32.12, 33.80, 34.18, 36.96, 37.76, 38.09, 38.91, 39.61, 39.68, 42.53, 46.02, 47.53, 52.60, 52.93, 56.49, 107.20, 118.94, 124.35, 127.37, 128.62, 138.54, 146.31, 160.13, 168.50, 170.60, 173.28, 184.82; IR (KBr, $cm^{-1}$): 3417, 3413, 2924, 2853, 1652, 1632, 1598, 1488, 1456, 1385, 1231, 1116, 1031, 844, 792; HRMS (ESI): *m/z* $[M+H]^+$ calcd for $C_{42}H_{60}N_3O_5$: 686.4533; found: 686.4514.

#### 4.2.9. 6′-Methoxy-4′,7′-dioxo-4′,7′-dihydro-1′H-ursa-2,12-dieno[3,2-b] indol-28- (2-benzoylhydrazide) (6h)

Red powder solid; M.p. 288 ~ 290 °C; Yield: 75%; $^1$H NMR (600 MHz, $CDCl_3$): $\delta$ 0.80 (s, 3H), 0.89 (s, 3H), 0.94 (d, $J$ = 5.9 Hz, 3H), 0.98 (d, $J$ = 5.2 Hz, 3H), 1.15 (s, 3H), 1.17 (s, 3H), 1.26 (s, 3H), 1.33 (m, 4H), 1.38 (d, $J$ = 13.2 Hz, 1H), 1.42 (d, $J$ = 9.1 Hz, 1H), 1.50 (m, 5H), 1.71 (m, 1H), 1.78 (m, 2H), 1.96 (d, $J$ = 13.7 Hz, 1H), 2.01 (m, 1H), 2.14 ~ 2.21 (m, 3H), 2.27 (m, 1H), 3.08 (d, $J$ = 16.5 Hz, 1H), 3.81 (s, 3H), 5.65 (s, 1H), 5.67 (brs, 1H), 7.45 (t, $J$ = 7.7 Hz, 2H), 7.53 (t, $J$ = 7.4 Hz, 1H), 7.79 (d, $J$ = 8.0 Hz, 2H), 9.23 (d, $J$ = 6.8 Hz, 1H), 9.29 (d, $J$ = 7.2 Hz, 1H); $^{13}$C NMR (150 MHz, DMSO-$d_6$): $\delta$ 16.06, 17.52, 17.57, 19.13, 21.60, 22.89, 23.44, 23.54, 23.99, 27.87, 30.34, 31.05, 32.69, 34.38, 37.42, 37.71, 38.27, 38.85, 39.28, 42.36, 45.93, 47.15, 52.27, 52.84, 55.34, 56.81, 107.01, 117.63, 123.44, 125.10, 127.96, 128.70, 128.97,

131.92, 133.46, 138.44, 146.30, 160.45, 165.97, 170.08, 176.03, 184.92; IR (KBr, $cm^{-1}$): 3444, 3340, 2925, 2869, 1641, 1595, 1632, 1490, 1452, 1382, 1334, 1268, 1231, 1115, 1030, 843, 792; HRMS (ESI): *m/z* $[M+H]^+$ calcd for $C_{44}H_{56}N_3O_5$: 706.4220; found: 706.4211.

#### *4.2.10. 6′-Methoxy-4′,7′-dioxo-4′,7′-dihydro-1′H-ursa-2,12-dieno[3,2-b] indol-28-[2-(4- methylbenzoyl)hydrazide] (**6i**)*

Red powder solid; M.p. 295 ~ 297 °C; Yield: 72%; $^1$H NMR (600 MHz, DMSO-$d_6$): $\delta$ 0.82 (s, 3H), 0.83 (s, 3H), 0.87 (d, $J$ = 6.4 Hz, 3H), 0.93 (d, $J$ = 5.8 Hz, 3H), 1.08 (s, 3H), 1.16 (s, 3H), 1.23 (m, 3H), 1.25 (s, 3H), 1.29 (m, 1H), 1.38 (m, 3H), 1.45 ~ 1.57 (m, 3H), 1.63 ~ 1.75 (m, 3H), 1.78 (d, $J$ = 8.4 Hz, 1H), 1.95 (m, 2H), 2.01 ~ 2.05 (m, 3H) 2.30 (d, $J$ = 11.0 Hz, 1H), 2.35 (s, 3H), 2.93 (d, $J$ = 16.3 Hz, 1H), 3.73 (s, 3H), 5.25 (t, $J$ = 3.1 Hz, 1H), 5.68 (s, 1H), 7.27 (d, $J$ = 8.1 Hz, 2H), 7.77 (d, $J$ = 8.1 Hz, 2H), 9.32 (s, 1H), 10.01 (s, 1H), 12.43 (s, 1H); $^{13}$C NMR (150 MHz, DMSO-$d_6$): $\delta$ 16.08, 17.54, 17.59, 19.12, 21.46, 21.62, 22.91, 23.43, 23.53, 23.95, 27.85, 30.34, 31.03, 31.62, 32.68, 34.38, 37.43, 37.70, 38.24, 38.86, 39.25, 42.35, 45.89, 47.12, 52.25, 52.79, 56.84, 107.01, 117.64, 123.41, 125.05, 127.98, 129.25, 130.61, 138.44, 141.88, 146.31, 147.24, 160.45, 165.83, 170.09, 176.07, 184.96; IR (KBr, $cm^{-1}$): 3418, 3257, 2925, 2855, 1664, 1641, 1597, 1490, 1448, 1385, 1262, 1231, 1114, 1027, 802, 745; HRMS (ESI): *m/z* $[M+H]^+$ calcd for $C_{45}H_{58}N_3O_5$: 720.4376; found: 720.4362.

#### *4.2.11. 6′-Methoxy-4′,7′-dioxo-4′,7′-dihydro-1′H-ursa-2,12-dieno[3,2-b] indol-28-[2-(3- pyridinylcarbonyl)hydrazide] (**6j**)*

Red powder solid; M.p. 285 ~ 287 °C; Yield: 74%; $^1$H NMR (600 MHz, $CDCl_3$): $\delta$ 0.80 (s, 3H), 0.89 (s, 6H), 0.95 (s, 3H), 1.12 (s, 3H), 1.22 (s, 3H), 1.24 ~ 1.29 (m, 3H), 1.31 (s, 3H), 1.36 (m, 1H), 1.38 ~ 1.61 (m, 7H), 1.65 ~ 1.77 (m, 3H), 1.85 (m, 1H), 1.98 ~ 2.12 (m, 3H), 2.15 (d, $J$ = 16.6 Hz, 2H), 2.22 (m, 1H), 3.07 (d, $J$ = 16.4 Hz, 1H), 3.76 (s, 3H), 5.59 (brs, 1H), 5.63 (s, 1H), 7.34 (t, $J$ = 5.9 Hz, 1H), 8.13 (s, 1H), 8.72 (s, 1H), 9.06 (s, 1H), 9.25 (s, 1H), 10.51 (brs, 1H); $^{13}$C NMR (150 MHz, $CDCl_3$) $\delta$ 15.92, 16.43, 17.09, 19.18, 21.14, 22.69, 23.24, 23.58, 24.93, 27.83, 30.19, 30.73, 31.43, 32.11, 34.21, 37.75, 38.07, 38.89, 39.59, 39.68, 42.57, 45.98, 47.86, 52.57, 52.96, 56.56, 107.15, 119.00, 119.09, 124.36, 127.39, 128.59, 128.83, 130.90, 135.96, 138.56, 146.52, 147.98, 160.15, 161.58, 170.61, 174.60, 184.91; IR (KBr, $cm^{-1}$): 3451, 3248, 2928, 2856, 1654, 1641, 1593, 1488, 1450, 1334, 1312, 1231, 1115, 1029, 842, 705; HRMS (ESI): *m/z* $[M+H]^+$ calcd for $C_{43}H_{55}N_4O_5$: 707.4172; found: 707.4172.

### *4.3. General procedures for the synthesis of compounds **6k-t***

The indoloquinone derivative **5** (0.1 mmol) was dissolved in 2 mL of dichloromethane, HOBT (18 mg, 0.12 mmol) and DCC (24 mg, 0.12 mmol) were added to the reaction system and the mixture was stirred at room temperature for 30 min. Then different 1,2-diaminoalkanes (0.12 mmol) were added, and the mixture was stirred at room temperature overnight. After the reaction was completed, DCU was filtered off. The filtrate was concentrated under reduced pressure. The acetonitrile was dissolved and left overnight. The DCU was further filtered off and concentrated under reduced pressure to remove the solvent. The residue was purified by silica gel chromatography (dichloromethane-methanol 200:1 ~ 50:1, v/v) to afford the corresponding amide derivatives **6k-t** in 67 ~ 78% yields.

#### *4.3.1. 6′-Methoxy-4′,7′-dioxo-4′,7′-dihydro-1′H-ursa-2,12-dieno[3,2-b] indol-28-amide (**6k**)*

Red powder solid; M.p. 278 ~ 280 °C; Yield: 72%; $^1$H NMR (400 MHz, DMSO-$d_6$): $\delta$ 0.82 (s, 3H), 0.83 (d, $J$ = 4.3 Hz, 3H), 0.85 (d, $J$ = 6.0 Hz, 3H), 0.92 (s, 3H), 1.07 (s, 3H), 1.15 (s, 3H), 1.24 (m, 2H), 1.25 (s, 3H), 1.28 ~ 1.36 (m, 4H), 1.40 ~ 1.48 (m, 4H), 1.59 (m, 3H), 1.69 (t, $J$ = 8.6 Hz, 1H), 1.82 (dd, $J$ = 12.6, 2.2 Hz, 1H), 1.88 (dd, $J$ = 13.2, 2.6 Hz, 1H), 1.97 (m, 2H), 2.04 (d, $J$ = 16.5 Hz, 1H), 2.15 (d, $J$ = 10.8 Hz, 1H), 2.92 (d, $J$ = 16.3 Hz, 1H), 3.73 (s, 3H), 5.29 (t, $J$ = 3.6 Hz, 1H), 5.68 (s, 1H), 6.71 (s, 2H), 12.43 (s, 1H); $^{13}$C NMR (100 MHz, DMSO-$d_6$): $\delta$ 16.00, 17.26, 17.56, 19.12, 21.23, 21.60, 22.53, 22.91, 23.46, 23.55, 24.10, 26.81, 27.91, 30.33, 34.37, 37.53, 37.70, 38.13, 38.95, 39.42, 42.31, 45.79, 47.16, 52.69, 52.72, 56.84, 107.01, 117.60, 121.44, 123.40, 124.90, 128.95, 138.89, 160.44, 170.09, 179.18, 184.95; IR (KBr, $cm^{-1}$): 3558, 3232, 2926, 2854, 1662, 1641, 1596, 1489, 1450, 1385, 1334, 1264, 1231, 1114, 1029, 842, 792; HRMS (ESI): *m/z* $[M+H]^+$ calcd for $C_{37}H_{51}N_2O_4$: 587.3849; found: 587.3850.

#### *4.3.2. 6′-Methoxy-4′,7′-dioxo-4′,7′-dihydro-N-methyl-1′H-ursa-2,12-dieno [3,2-b]indol-28-amide (**6l**)*

Red powder solid; M.p. 287 ~ 289 °C; Yield: 74%; $^1$H NMR (600 MHz, $CDCl_3$): $\delta$ 0.82 (s, 3H), 0.88 (dd, $J$ = 6.4, 1.9 Hz, 3H), 0.90 (s, 3H), 0.94 (s, 3H), 1.11 (s, 3H), 1.23 (s, 3H), 1.25 ~ 1.29 (m, 2H), 1.30 (s, 3H), 1.32 (m, 1H), 1.36 ~ 1.50 (m, 5H), 1.51 ~ 1.64 (m, 3H), 1.77 (m, 2H), 1.87 (d, $J$ = 10.8 Hz, 1H), 1.91 (m, 1H), 1.96 (m, 1H), 2.02 (m, 1H), 2.07 (m, 1H), 2.15 (d, $J$ = 16.4 Hz, 1H), 2.22 (m, 1H), 2.73 (d, $J$ = 4.6 Hz, 3H), 3.06 (d, $J$ = 16.4 Hz, 1H), 3.79 (s, 3H, $OCH_3$), 5.39 (brs, 1H), 5.65 (s, 1H) , 5.98 (m, 1H), 10.13 (s, 1H); $^{13}$C NMR (150 MHz, $CDCl_3$) $\delta$ 15.81, 16.38, 17.25, 19.07, 21.23, 23.18, 23.23, 23.50, 25.00, 26.28, 27.85, 30.66, 30.92, 32.00, 34.16, 36.90, 37.78, 38.01, 39.13, 39.48, 39.90, 42.66, 45.98, 47.83, 52.57, 53.97, 56.50, 107.12, 118.63, 124.16, 125.71, 128.71, 139.95, 146.05, 160.18, 168.52, 178.83, 185.12; IR (KBr, $cm^{-1}$): 3445, 3209, 2935, 2852, 1667, 1644, 1594, 1493, 1448, 1384, 1231, 1113, 1029, 843, 792; HRMS (ESI): *m/z* $[M+H]^+$ calcd for $C_{38}H_{53}N_2O_4$: 601.4005; found: 601.4005.

#### *4.3.3. 6′-Methoxy-4′,7′-dioxo-4′,7′-dihydro-N-ethyl-1′H-ursa-2,12-dieno [3,2-b]indol-28-amide (**6m**)*

Red powder solid; M.p. 279 ~ 281 °C; Yield: 71%; $^1$H NMR (600 MHz, $CDCl_3$): $\delta$ 0.86 (s, 3H), 0.89 (d, $J$ = 6.4 Hz, 3H), 0.91 (s, 3H), 0.94 (s, 3H), 1.09 (t, $J$ = 7.3 Hz, 3H), 1.11 (s, 3H), 1.22 (s, 3H), 1.28 (m, 1H), 1.30 (s, 3H), 1.31 (m, 2H), 1.38 ~ 1.49 (m, 4H), 1.57 (m, 2H), 1.67 (m, 2H), 1.75 (m, 2H), 1.89 (m, 3H), 1.97 (dd, $J$ = 13.6, 3.8 Hz, 1H), 2.05 (m, 1H), 2.15 (d, $J$ = 14.4 Hz, 1H), 2.21 (dt, $J$ = 18.4, 5.0 Hz, 1H), 3.06 (d, $J$ = 4.4 Hz, 1H), 3.13 (m, 1H), 3.29 (m, 1H), 3.79 (s, 3H, $OCH_3$), 5.39 (t, $J$ = 3.7 Hz, 1H), 5.65 (s, 1H), 5.88 (t, $J$ = 5.1 Hz, 1H), 10.21(s, 1H); $^{13}$C NMR (150 MHz, $CDCl_3$): $\delta$ 14.53, 15.86, 16.73, 17.23, 19.07, 21.22, 23.09, 23.20, 23.53, 24.98, 27.89, 30.66, 30.97, 32.21, 34.18, 34.36, 37.10, 37.78, 38.07, 39.12, 39.57, 39.92, 42.77, 45.98, 47.68, 52.61, 54.14, 56.51, 107.12, 118.74, 124.17, 125.70, 128.70, 139.79, 146.12, 160.17, 170.44, 177.98, 185.08; IR (KBr, $cm^{-1}$): 3333, 3208, 2930, 2851, 1665, 1629, 1595, 1490, 1449, 1259, 1232, 1115, 1031, 841, 792; HRMS (ESI): *m/z* $[M+H]^+$ calcd for $C_{39}H_{55}N_2O_4$: 615.4162; found: 615.4161.

#### *4.3.4. 6′-Methoxy-4′,7′-dioxo-4′,7′-dihydro-N-propyl-1′H-ursa-2,12-dieno [3,2-b]indol-28-amide (**6n**)*

Red powder solid; M.p. 285 ~ 287 °C; Yield: 71%; $^1$H NMR (600 MHz, $CDCl_3$): $\delta$ 0.84 (s, 3H), 0.88 ~ 0.91 (m, 9H), 0.94 (s, 3H), 1.11 (s, 3H), 1.22 (s, 3H), 1.23 ~ 1.28 (m, 3H), 1.30 (s, 3H), 1.31 (m, 1H), 1.38 ~ 1.51 (m, 7H), 1.56 (m, 2H), 1.66 (td, $J$ = 13.4, 3.3 Hz, 1H), 1.75 (m, 2H), 1.88 (d, $J$ = 16.5 Hz, 2H), 1.96 (td, $J$ = 13.7, 3.8 Hz, 1H), 2.05 (m, 1H), 2.15 (d, $J$ = 16.5 Hz, 1H), 2.21 (dt, $J$ = 18.2, 5.3 Hz, 1H), 2.98 (m, 1H), 3.07 (d, $J$ = 16.4 Hz, 1H), 3.28 (m, 1H), 3.79 (s, 3H), 5.38 (t, $J$ = 3.6 Hz, 1H), 5.65 (s, 1H), 5.94 (d, $J$ = 5.2 Hz, 1H), 10.17 (s, 1H); $^{13}$C NMR (150 MHz, $CDCl_3$) $\delta$ 11.58, 15.86, 16.76, 17.22, 19.07, 21.22, 22.52, 23.10, 23.23, 23.52, 24.90, 27.88, 30.68, 30.98, 32.23, 34.17, 37.20, 37.78, 38.05, 39.12, 39.56, 39.92, 41.23, 42.77, 45.98, 47.85, 52.59, 54.22, 56.51, 107.13, 118.77, 124.20, 125.66, 128.67, 139.82, 146.13, 160.17, 170.46, 178.03, 185.07; IR (KBr, $cm^{-1}$): 3431, 3220, 2927, 2869, 1667, 1642, 1597, 1490, 1451, 1385, 1335, 1231, 1115, 1031, 842, 792; HRMS (ESI): *m/z* $[M+H]^+$ calcd for $C_{40}H_{57}N_2O_4$: 629.4318; found: 629.4318.

*4.3.5. 6′-Methoxy-4′,7′-dioxo-4′,7′-dihydro-N,N-dimethyl-1′H-ursa-2,12-dieno[3,2-b]indol-28- amide (**6o**)*

Red powder solid; M.p. 269 ~ 271 °C; Yield: 67%; $^1$H NMR (400 MHz, $CDCl_3$): $\delta$ 0.81 (s, 3H), 0.89 (m, 6H), 0.94 (d, $J$ = 6.4 Hz, 3H), 1.10 (s, 3H), 1.20 (s, 3H), 1.26 (m, 2H), 1.28 (s, 3H), 1.32 (m, 2H), 1.38 ~ 1.53 (m, 4H), 1.64 (m, 1H), 1.75 (m, 2H), 1.85 (d, $J$ = 14.1 Hz, 2H), 2.00 (m, 2H), 2.09 ~ 2.25 (m, 4H), 2.54 (d, $J$ = 11.0 Hz, 1H), 3.00 (s, 6H), 3.06 (d, $J$ = 16.5 Hz, 1H), 3.80 (s, 3H), 5.31 (t, $J$ = 3.6 Hz, 1H), 5.65 (s, 1H), 9.73 (s, 1H); $^{13}$C NMR (100 MHz, $CDCl_3$): $\delta$ 15.74, 16.65, 17.35, 19.11, 21.26, 23.40, 23.78, 27.22, 28.01, 29.32, 30.61, 30.81, 32.37, 34.02, 34.08, 37.88, 37.94, 38.72, 38.87, 39.36, 42.38, 42.71, 46.11, 48.74, 52.22, 52.63, 56.53, 107.21, 119.07, 124.29, 128.55, 129.91, 137.47, 146.05, 160.05, 170.54, 176.39, 184.89; IR (KBr, cm$^{-1}$): 3418, 3217, 2924, 2850, 1667, 1643, 1594, 1490, 1447, 1384, 1259, 1229, 1114, 1029, 842, 792; HRMS (ESI): *m/z* $[M+H]^+$ calcd for $C_{39}H_{55}N_2O_4$: 615.4162; found: 615.4161.

*4.3.6. 6′-Methoxy-4′,7′-dioxo-4′,7′-dihydro-N,N-diethyl-1′H-ursa-2,12-dieno[3,2-b]indol-28- amide (**6p**)*

Red powder solid; M.p. 270 ~ 272 °C; Yield: 76%; $^1$H NMR (600 MHz, $CDCl_3$): $\delta$ 0.85 (s, 3H), 0.89 (d, $J$ = 5.9 Hz, 3H), 0.90 (s, 3H), 0.93 (d, $J$ = 6.2 Hz, 3H), 1.10 (s, 3H), 1.12 (brs, 6H), 1.19 (s, 3H), 1.25 (m, 2H), 1.28 (s, 3H), 1.30 (m, 2H), 1.35 ~ 1.60 (m, 8H), 1.66 ~ 1.90 (m, 6H), 2.00 ~ 2.20 (m, 4H), 3.07 (d, $J$ = 16.5 Hz, 1H), 3.21 (brs, 2H), 3.80 (s, 3H, $OCH_3$), 5.33 (s, 1H), 5.65 (s, 1H), 9.58 (s, 1H); $^{13}$C NMR (150 MHz, $CDCl_3$): $\delta$ 14.08, 15.87, 16.85, 17.46, 19.09, 21.01, 23.25, 23.41, 23.54, 24.94, 28.43, 30.57, 30.86, 32.58, 33.93, 34.11, 36.70, 37.86, 38.11, 38.74, 39.18, 39.77, 42.49, 45.98, 49.24, 52.70, 53.18, 56.49, 107.22, 118.74, 124.20, 125.76, 128.79, 139.13, 145.77, 160.06, 170.53, 173.34, 184.84; IR (KBr, cm$^{-1}$): 3431, 3222, 2928, 2868, 1666, 1644, 1597, 1490, 1452, 1385, 1231, 1114, 1030, 841, 792; HRMS (ESI): *m/z* $[M+H]^+$ calcd for $C_{41}H_{59}N_2O_4$: 643.4475; found: 643.4479.

*4.3.7. 6′-Methoxy-4′,7′-dioxo-4′,7′-dihydro-N,N-dipropyl-1′H-ursa-2,12-dieno[3,2-b]indol-28- amide (**6q**)*

Red powder solid; M.p. 278 ~ 280 °C; Yield: 72%; $^1$H NMR (600 MHz, $CDCl_3$): $\delta$ 0.85 (s, 3H), 0.88 ~ 0.91 (m, 12H), 0.94 (s, 3H), 1.11 (s, 3H), 1.23 (s, 3H), 1.28 (m, 2H), 1.30 (s, 3H), 1.31 (m, 2H), 1.37 ~ 1.60 (m, 10*H*), 1.68 (m, 2H), 1.76 (m, 2H), 1.80 ~ 2.00 (m, 4H), 2.05 (m, 2H), 2.15 (d, $J$ = 16.5 Hz, 1H), 2.21 (dt, $J$ = 18.3, 4.9 Hz, 1H), 3.00 (m, 1H), 3.07 (d, $J$ = 16.4 Hz, 1H), 3.30 (m, 1H), 3.79 (s, 3H, $OCH_3$), 5.38 (brs, 1H), 5.65 (s, 1H), 10.19 (s, 1H); $^{13}$C NMR (150 MHz, $CDCl_3$): $\delta$ 11.56, 15.84, 16.76, 17.21, 19.08, 21.19, 22.52, 23.11, 23.18, 23.53, 24.91, 27.90, 30.65, 30.98, 32.25, 34.19, 37.22, 37.79, 38.08, 39.12, 39.58, 39.92, 41.24, 42.77, 46.00, 47.86, 52.65, 54.23, 56.47, 107.13, 118.72, 124.18, 125.66, 128.72, 139.82, 146.10, 160.18, 170.43, 177.98, 185.05; IR (KBr, cm$^{-1}$): 3417, 3217, 2937, 2868, 1667, 1648, 1594, 1491, 1452, 1385, 1232, 1115, 1032, 841, 790; HRMS (ESI): *m/z* $[M+H]^+$ calcd for $C_{43}H_{63}N_2O_4$: 671.4788; found: 671.4797.

*4.3.8. 6′-Methoxy-4′,7′-dioxo-4′,7′-dihydro-N-[2-(dimethylamino)ethyl]-1′H-ursa-2,12-dieno [3,2-b]indol-28-amide (**6r**)*

Red powder solid; M.p. 332 ~ 335 °C; Yield: 78%; $^1$H NMR (600 MHz, $CDCl_3$): $\delta$ 0.87 (s, 3H), 0.89 (d, $J$ = 7.1 Hz, 3H), 0.90 (s, 3H), 0.94 (d, $J$ = 6.1 Hz, 3H), 1.11 (s, 3H), 1.22 (s, 3H), 1.30 (s, 3H), 1.32 (m, 2H), 1.37 ~ 1.51 (m, 6H), 1.56 (m, 2H), 1.69 (t, $J$ = 13.14 Hz, 1H), 1.76 (m, 2H), 1.89 (m, 2H), 1.92 ~ 2.08 (m, 3H), 2.17 (m, 2H), 2.21 (s, 6H), 2.36 (dd, $J$ = 7.2 Hz, 5.5 Hz, 2H), 3.08 (d, $J$ = 16.4 Hz, 1H), 3.16 (m, 1H), 3.31 (m, 1H), 3.79 (s, 3H), 5.36 (s, 1H), 5.64 (s, 1H), 6.51 (s, 1H), 10.20 (s, 1H); $^{13}$C NMR (150 MHz, $CDCl_3$): $\delta$ 15.82, 16.80, 17.12, 19.10, 21.13, 23.10, 23.22, 23.55, 24.84, 27.96, 30.66, 31.02, 32.35, 34.17, 36.91, 37.23, 37.81, 38.09, 39.10, 39.65, 39.88, 42.68, 45.22, 46.05, 47.89, 52.74, 54.25, 56.41, 57.64, 107.13, 118.75, 124.22, 125.94, 128.73, 139.05, 146.12, 160.19, 170.47, 178.02, 184.95; IR (KBr, cm$^{-1}$): 3390, 3227, 2924, 2857, 1649, 1642, 1596, 1489, 1450, 1385, 1231, 1115, 1030, 842, 792; HRMS (ESI): *m/z* $[M+H]^+$ calcd for $C_{41}H_{60}N_3O_4$: 658.4584; found: 658.4579.

*4.3.9. 6′-Methoxy-4′,7′-dioxo-4′,7′-dihydro-N-[3-(dimethylamino) propyl]-1′H-ursa-2,12-dieno [3,2-b]indol-28-amide (**6s**)*

Red powder solid; M.p. 285 ~ 287 °C; Yield: 75%; $^1$H NMR (400 MHz, $CDCl_3$): $\delta$ 0.81 (s, 3H), 0.87 ~ 0.91 (m, 6H), 0.94 (d, $J$ = 6.4 Hz, 3H), 1.10 (s, 3H), 1.21 (s, 3H), 1.27 (m, 2H), 1.29 (s, 3H), 1.38 ~ 1.60 (m, 8H), 1.67 ~ 1.81 (m, 4H), 1.87 (m, 2H), 1.96 ~ 2.07 (m, 4H), 2.14 (d, $J$ = 16.8 Hz, 1H), 2.20 (m, 1H), 2.56 (s, 6H), 2.74 (m, 2H), 3.06 (d, $J$ = 16.5 Hz, 1H), 3.15 (m, 1H), 3.42 (m, 1H), 3.80 (s, 3H), 5.41 (t, $J$ = 3.5 Hz, 1H), 5.64 (s, 1H), 6.85 (t, $J$ = 5.0 Hz, 1H), 9.96 (s, 1H); $^{13}$C NMR (100 MHz, $CDCl_3$): $\delta$ 15.81, 16.81, 17.18, 19.08, 21.21, 23.27, 23.36, 23.44, 24.65, 25.20, 27.85, 30.78, 30.96, 32.21, 34.12, 37.21, 37.60, 37.80, 37.96, 39.00, 39.57, 39.74, 42.51, 43.87, 45.96, 47.80, 52.55, 53.50, 56.46, 56.53, 107.16, 118.84, 124.23, 125.76, 128.59, 139.00, 146.09, 160.10, 170.51, 178.63, 184.95; IR (KBr, cm$^{-1}$): 3433, 3224, 2925, 2853, 1662, 1644, 1597, 1489, 1449, 1260, 1230, 1113, 1029, 842, 804; HRMS (ESI): *m/z* $[M+H]^+$ calcd for $C_{42}H_{62}N_3O_4$: 672.4740; found: 672.4742.

*4.3.10. 6′-Methoxy-4′,7′-dioxo-4′,7′-dihydro-N-[4-(dimethylamino) butyl]-1′H-ursa-2,12-dieno [3,2-b]indol-28-amide (**6t**)*

Red powder solid; M.p. 307 ~ 309 °C; Yield: 72%; $^1$H NMR (600 MHz, $CDCl_3$): $\delta$ 0.84 (s, 3H), 0.89 (d, $J$ = 6.4 Hz, 3H), 0.91 (s, 3H), 0.95 (brs, 3H), 1.11 (s, 3H), 1.20 (s, 3H), 1.25 (m, 2H), 1.28 (s, 3H), 1.31 (m, 2H), 1.41 ~ 1.60 (m, 11*H*), 1.67 (td, $J$ = 13.3, 3.2 Hz, 1H), 1.75 (m, 2H), 1.86 (d, $J$ = 12.8 Hz, 1H), 1.91 (d, $J$ = 10.4 Hz, 1H), 1.97 (m, 1H), 2.06 (m, 1H), 2.16 (d, $J$ = 16.5 Hz, 1H), 2.22 (dt, $J$ = 18.4, 4.0 Hz, 1H), 2.30 (s, 6H), 2.40 (m, 2H), 3.04 (m, 1H), 3.07 (d, $J$ = 16.4 Hz, 1H), 3.35 (m, 1H), 3.81 (s, 3H), 5.39 (s, 1H), 5.65 (s, 1H), 6.12 (t, $J$ = 4.9 Hz, 1H), 9.51 (s, 1H); $^{13}$C NMR (150 MHz, $CDCl_3$): $\delta$ 15.84, 16.72, 17.19, 19.07, 21.21, 23.14, 23.19, 23.50, 24.39, 24.81, 27.03, 27.86, 30.64, 30.94, 32.19, 34.19, 37.26, 37.76, 38.05, 39.02, 39.06, 39.55, 39.85, 42.67, 44.89, 45.96, 47.77, 52.62, 53.95, 56.50, 58.78, 107.09, 118.72, 124.20, 125.67, 128.69, 139.61, 144.00, 160.16, 170.40, 178.14, 185.09; IR (KBr, cm$^{-1}$): 3417, 3223, 2925, 2854, 1662, 1641, 1596, 1491, 1452, 1230, 1261, 1114, 1030, 842, 793; HRMS (ESI): *m/z* $[M+H]^+$ calcd for $C_{43}H_{64}N_3O_4$: 686.4897; found: 686.4901.

### *4.4. MTT assay*

Human breast cancer cell line (MCF-7), human cervical carcinoma cell line (HeLa), human hepatocarcinoma cell line (HepG2) and human normal gastric mucosal cell line (Ges-1) were maintained in Dulbecco Modified Eagle Medium (DMEM) containing 4.0 mM L-Glutamine and 4500 mg/l Glucose supplemented with 10% (v/v) foetalbovine serum (FBS) and 100 unites/mL penicillin/streptomycin at 37 °C in humidified atmosphere of 5% $CO_2$ and 95% air.

Cytotoxic activities of the indolequinone Derivative of UA were determined *in vitro* cytotoxic activities against the aforementioned cell lines via the typical MTT colorimetric method. Briefly, exponentially growing cells were seeded into 96-well (100 mL/well at a density of 2 × $10^5$ cells/mL). After 24 h incubation at 37 °C and 5% $CO_2$ to allow cell attachment, and treated with different concentrations of the synthetic compounds for 72 h, and then 100 mL of MTT (10 mg/mL) was added and incubation for 3 ~ 4 h at 37 °C, the purple formazan crystals (a reduced form of MTT) generated in viable cells were dissolved by adding 100 mL DMSO to each well. The plates were swirled gently for 5 min to dissolve the precipitate and quantified by measuring the OD of the plates at the wavelength of 540 nm. Each concentration was repeated in three wells and the same experimental conditions were maintained for all testing procedures. The MTT assays were repeated three times for each cell line. The results were expressed as $IC_{50}$ values (mean, n = 3) with standard deviations, which was defined as the concentration at which 50% survival of cells was discerned. Etoposide was co-assayed as positive control.

### 4.5. Cell cycle analysis

Cell cycle distributions in MCF-7 cells were determined through PI staining and analysed by flow cytometry [54]. MCF-7 cells were seeded into a six-well plate at $5 \times 10^5$ cell/mL and treated with different concentrations of compound **6t** for 48 h. After treatment, cells were detached with 0.25% trypsin, harvested by centrifugation, washed twice with ice-cold PBS and then fixed and permeabilised with ice-cold 70% ethanol at 4 °C overnight. Ethanol was removed and the cells were washed twice with ice-cold PBS. After this, the cells were treated with 100 μL of RNase (100 μg/mL) at 37 °C for 30 min, followed by incubation with 400 μL of DNA staining solution propidium iodide (PI) (1 mg/mL) in the dark at 4 °C for 30 min. The samples were analysed by a flow cytometer (BectonDickinson FACSCalibur, Totowa, NJ, USA) and data were analysed using the FlowJo software (Becton-Dickinson & Co, Totowa, NJ, USA).

### 4.6. Wound healing assay

MCF-7 cells ($5 \times 10^5$ cells/well) were grown in a 12-well plate for 24 h. Scratches were made in confluent monolayers using 200 μL pipette tip. Then, wounds were washed twice with PBS to remove non-adherent cell debris. The media containing different concentrations (0, 2, 4 and 6 μM) of compound **6t** were added to the corresponding wells. Cells which migrated across the wound area were photographed under the phase contrast microscope (Olympus 1X71 Inverted System Microscope, Olympus, Japan) after 24 and 48 h treatment.

### 4.7. Cell apoptosis analysis

The extent of apoptosis was quantitatively measured using Annexin V-FITC/PI dual staining assay [55]. MCF-7 cells were seeded into a six-well plate at $5 \times 10^5$ cells per well in 10% foetal calf serum (FBS)-DMEM into six-well plates and treated with different concentrations of the indicated compound **6t** for 48 h. The cells were detached with 0.25% trypsin, washed with ice-cold PBS for twice and then resuspended in 1 × Binding buffer (0.1 M Hepes/ NaOH (pH 7.4), 1.4 M NaCl, 25 mM $CaCl_2$). The cells were stained with 5 μL of Annexin V-FITC and 5 μL of PI (propidium indole) to each tube. The cells were gently vortexed and incubated in the dark at room temperature for 15 min and then keep them at 4 °C. The samples were analysed by a flow cytometer (Becton-Dickinson FACSCalibur, Totowa, NJ, USA) and data were analysed using the FlowJo software.

### 4.8. ROS generation assay

ROS generation assay was performed by using the reactive oxygen species assay kit (Beyotime Biotech., Nantong, China). Intracellular ROS generation was tested through dichlorodihydro fluorescein diacetate (DCFH-DA) assay [56]. DCFH-DA is taken up by MCF-7 cells, and then activated by esterase-mediated cleavage of acetate to form DCFH, which is trapped in the cells. DCFH is converted to fluorescein DCF in the presence of ROS. MCF-7 cells were seeded in six-well plates and incubated with different concentrations of compound **6t** for 48 h. After removing the compound solution, cells were treated with 10 μM of DCFH-DA at 37 °C for 20 min. Subsequently, the cells were washed with PBS for three times and then exposed to light. Immediately after light exposure, the fluorescence intensity of dichlorofluorescein (DCF) was measured with excitation at 488 nm and emission at 525 nm by a flow cytometry (Becton-Dickinson FACSCalibur, Totowa, NJ, USA).

### 4.9. JC-1 mitochondrial membrane potential assay

The JC-1 mitochondrial membrane potential assay kit (Keygene Biotech., Nanjing, China) was employed to measure mitochondrial depolarisation in MCF-7 cells. Briefly, cells cultured in six-well plates after indicated treatments by compound **6t** were incubated with an equal volume of JC-1 staining solution (5 μg/mL) at 37 °C for 20 min and rinsed twice with PBS. Mitochondrial membrane potentials were monitored by determining the relative amounts of dual emissions from mitochondrial JC-1 monomers or aggregates using flow cytometry (Becton-Dickinson FACSCalibur, New York, NY, USA). Mitochondrial membrane depolarisation is indicated by an increase in the percentage of cells with low ΔΨm (green fluorescence, lower right quadrant) compared with cells with high ΔΨm (red fluorescence, upper right quadrant).

### 4.10. Western blot analysis

MCF-7 cells were seeded at a density of $5 \times 10^6$ cells per well and attached for 8 h, and then treated with different concentrations of compound **6t** for 48 h. After the treatment, the cells were harvested and washed twice with PBS. The harvested cells were lysed with radioimmunoprecipitation assay (RIPA) lysis buffer (Beyotime Biotech., Nantong, China) with 1% cocktail (Sigma-Aldrich, St. Louis, MO, USA). Whole-cell protein lysates were prepared and centrifuged at 12,000 rpm for 10 min at 4 °C. The total proteins were determined using Bradford reagent (Bio-Rad Laboratories, Inc., Hercules, CA, USA). Exactly 40 μg of protein per lane was separated through sodium dodecyl sulphate–polyacrylamide gel electrophoresis and then transferred onto a polyvinylidene difluoride membrane (Millipore, Bedford, MA, USA). The membranes were incubated with each antibody and detected through immunoblot analysis. All of the antibodies were purchased from Cell signalling Technology, Inc. (Boston, MA, USA) and diluted in accordance with the manufacturer's instruction. Proteins were visualised using a C-Digit® imaging system (LI-COR, Lincoln, NE, USA).

## Declaration of Competing Interest

The authors declare that they have no known competing financial interests or personal relationships that could have appeared to influence the work reported in this paper.

## Acknowledgements

This work was supported by the National Natural Science Foundation of China (31770616), the Natural Science Foundation for Colleges and Universities in Jiangsu Province (17KJA220002) and Top-notch Academic Programs Project of Jiangsu Higher Education Institutions (PPZY2015C221). The authors are grateful to the Advanced Analysis & Testing Center of Nanjing Forestry University for the measurements of spectroscopic data.

## Appendix A. Supplementary data

Supplementary data to this article can be found online at https://doi.org/10.1016/j.bioorg.2021.104705.

## References

[1] F. Bray, J. Ferlay, I. Soerjomataram, R.L. Siegel, L.A. Torre, A. Jemal, Global cancer statistics 2018: GLOBOCAN estimates of incidence and mortality worldwide for 36 cancers in 185 countries, CA Cancer J. Clin. 68 (2018) 394–424.
[2] D.Y. Seo, S.R. Lee, J.W. Heo, M.H. No, B.D. Rhee, K.S. Ko, H.B. Kwak, J. Han, Ursolic acid in health and disease, Korean J. Physiol. Pharmacol. 22 (2018) 235–248.
[3] K. Nurgali, R.T. Jagoe, R. Abalo, Editorial: adverse effects of cancer chemotherapy: anything new to improve tolerance and reduce sequelae? Front. Pharmacol. 9 (2018) 245.
[4] D. Woods, J.J. Turchi, Chemotherapy induced DNA damage response: convergence of drugs and pathways, Cancer Biol. Ther. 14 (2013) 379–389.
[5] D.J. Newman, G.M. Cragg, Natural products as sources of new drugs from 1981 to 2014, J. Nat. Prod. 79 (2016) 629–661.

[6] J. Hodon, L. Borkova, J. Pokorny, A. Kazakova, M. Urban, Design and synthesis of pentacyclic triterpene conjugates and their use in medicinal research, Eur. J. Med. Chem. 182 (2019), 111653.
[7] M.K. Shanmugam, X. Dai, A.P. Kumar, B.K. Tan, G. Sethi, A. Bishayee, Ursolic acid in cancer prevention and treatment: molecular targets, pharmacokinetics and clinical studies, Biochem. Pharmacol. 85 (2013) 1579–1587.
[8] G. Kuttan, P. Pratheeshkumar, K.A. Manu, R. Kuttan, Inhibition of tumor progression by naturally occurring terpenoids, Pharm. Biol. 49 (2011) 995–1007.
[9] T. Zhou, Z. Li, O.H. Kang, S.H. Mun, Y.S. Seo, R. Kong, D.W. Shin, X.Q. Liu, D. Y. Kwon, Antimicrobial activity and synergism of ursolic acid 3-O-α-L-arabinopyranoside with oxacillin against methicillin-resistant *Staphylococcus aureus*, Int. J. Mol. Med. 40 (2017) 1285–1293.
[10] M. Tohmé, M. Gimenez, A. Peralta, M. Colombo, L.R. Delgui, Ursolic acid: A novel antiviral compound inhibiting rotavirus infection in vitro, Int. J. Antimicrob. Ag. 54 (2019) 601–609.
[11] S.N. Rai, W. Zahra, S.S. Singh, H. Birla, C. Keswani, H. Dilnashin, A.S. Rathore, R. Singh, R.K. Singh, S. Singh, Anti-inflammatory activity of ursolic acid in MPTP-induced parkinsonian mouse model, Neurotox. Res. 36 (2019) 452–462.
[12] P. Wu, T. Huang, D. Li, Q. Hu, A. Cheng, Z. Jiang, L. Jiao, S. Zhao, K. Zhang, Synthesis and evaluation of novel triterpene analogues of ursolic acid as potential antidiabetic agent, PLoS ONE 10 (2015), e0138767.
[13] M.S.A. Khan, S.U.K. Khundmiri, S.R. Khundmiri, M.M. Al-Sanea, P.L. Mok, Fruit-derived polysaccharides and terpenoids: Recent update on the gastroprotective effects and mechanisms, Front. Pharmacol. 9 (2018) 569.
[14] H.J. Fu, Y.R. Zhou, B.H. Bao, M.X. Jia, Y. Zhao, L. Zhang, J.X. Li, H. He, X. Zhou, Tryptophan hydroxylase 1 (Tph-1)-targeted bone anabolic agents for osteoporosis, J. Med. Chem. 57 (2014) 4692–4709.
[15] A.B. Ramos-Hryb, F.L. Pazini, M.P. Kaster, A.L.S. Rodrigues, Therapeutic potential of ursolic acid to manage neurodegenerative and psychiatric diseases, CNS Drugs 31 (2017) 1029–1041.
[16] M.H. Ghante, P.G. Jamkhande, Role of pentacyclic triterpenoids in chemoprevention and anticancer treatment: An overview on targets and underling mechanisms, J. Pharmacopunct. 22 (2019) 55–67.
[17] W. Jiang, R.Z. Huang, J. Zhang, T. Guo, M.T. Zhang, X.C. Huang, B. Zhang, Z. X. Liao, J. Sun, H.S. Wang, Discovery of antitumor ursolic acid long-chain diamine derivatives as potent inhibitors of NF-κB, Bioorg. Chem. 79 (2018) 265–276.
[18] K.Q. Chi, Z.Y. Wei, K.S. Wang, J. Wu, W.Q. Chen, X.J. Jin, H.R. Piao, Design, synthesis, and evaluation of novel ursolic acid derivatives as HIF-1α inhibitors with anticancer potential, Bioorg. Chem. 75 (2017) 157–169.
[19] Y.N. Song, P. Zhan, Q.Z. Zhang, X.Y. Liu, Privileged scaffolds or promiscuous binders: a glance of pyrrolo[2,1-f][1,2,4]triazines and related bridgehead nitrogen heterocycles in medicinal chemistry, Curr. Pharmaceut. Des. 19 (2013) 1528–1548.
[20] W. Caneschi, K.B. Enes, C.C. de Mendonca, F.D. Fernandes, F.B. Miguel, J. D. Martins, M. Le Hyaric, R.R. Pinho, L.M. Duarte, M.A.L. de Oliveira, H.F. Dos Santos, M.T.P. Lopes, D. Dittz, H. Silva, M.R.C. Couri, Synthesis and anticancer evaluation of new lipophilic 1,2,4 and 1,3,4-oxadiazoles, Eur. J. Med. Chem. 165 (2019) 18–30.
[21] Z.Y. Wei, K.Q. Chi, K.S. Wang, J. Wu, L.P. Liu, H.R. Piao, Design, synthesis, evaluation, and molecular docking of ursolic acid derivatives containing a nitrogen heterocycle as anti-inflammatory agents, Bioorg. Med. Chem. Letters. 28 (2018) 1797–1803.
[22] R.D. Taylor, M. MacCoss, A.D.G. Lawson, Rings in Drugs, J. Med. Chem. 57 (2014) 5845–5859.
[23] T.O.C. Leite, J.S. Novais, B.L.C. de Carvalho, V.F. Ferreira, L.A. Miceli, L. Fraga, B. Abrahim-Vieira, C.R. Rodrigues, A.M.S. Figueiredo, H.C. Castro, A.C. Cunha, Synthesis, in vitro and in silico studies of indolequinone derivatives against clinically relevant bacterial pathogens, Curr. Top. Med. Chem. 20 (2020) 192–208.
[24] M. Ye, Y. Wang, G.Y. Guo, Y.L. He, Y. Lu, Y.W. Ye, Q.H. Yang, P.Z. Yang, Physicochemical characteristics and antioxidant activity of arginine-modified melanin from Lachnum YM-346, Food Chem. 135 (2012) 2490–2497.
[25] S. Rockwell, I.T. Dobrucki, E.Y. Kim, S.T. Marrison, V.T. Vu, Hypoxia and radiation therapy: past history, ongoing research, and future promise, Curr. Mol. Med. 9 (2009) 442–458.
[26] S.P. Tan, A.M. Ali, M.A. Nafiah, K. Awang, K. Ahmad, Isolation and cytotoxic investigation of new carbazole alkaloids from *Murraya koenigii* (Linn.) Spreng, Tetrahedron 71 (2015) 3946–3953.
[27] V. Sofifiyev, J.P. Lumb, M. Volgraf, D. Trauner, Total synthesis of exiguamines A and B inspired by catecholamine chemistry, Chem. Eur. J. 18 (2012) 4999–5005.
[28] N.K. Utkina, A.E. Makarchenko, V.A. Denisenko, Zyzzyanones B–D, Dipyrroloquinones from the Marine Sponge *Zyzzya fuliginosa*, J. Nat. Prod. 68 (2005) 1424–1427.
[29] H. Oka, T. Yoshinari, T. Murai, K. Kuwamura, F. Satoh, K. Funaishi, A. Okura, H. Suda, M. Okanishi, Y. Shizuri, A new topoisomerase-II inhibitor, BE-10988, produced by a streptomycete, J. Antibiot. 44 (1991) 486–491.
[30] R.M. Phillips, H.R. Hendriks, G.J. Peters, EO9 (Apaziquone): from the clinic to the laboratory and back again, Br. J. Pharmacol. 168 (2013) 11–18.
[31] P. Wang, J. Wang, T.T. Guo, Y.X. Li, Synthesis and cytotoxic activity of the *N*-acetylglucosamine-bearing triterpenoid saponins, Carbohyd. Res. 345 (2010) 607–620.
[32] I.J. Jin, Y.I. Ko, Y.M. Kim, S.K. Han, Solubilization of oleanolic acid and ursolic acid by cosolvency, Arch. Pharm. Res. 20 (1997) 269–274.
[33] K.K. Bai, Z. Yu, F.L. Chen, F. Li, W.Y. Li, Y.H. Guo, Synthesis and evaluation of ursolic acid derivatives as potent cytotoxic agents, Bioorg. Med. Chem. Lett. 22 (2012) 2488–2493.
[34] S. Senkardes, N. Kaushik-Basu, I. Durmaz, D. Manvar, A. Basu, R. Atalay, S. G. Kucukguzel, Synthesis of novel diflunisal hydrazide-hydrazones as anti-hepatitis C virus agents and hepatocellular carcinoma inhibitors, Eur. J. Med. Chem. 108 (2016) 301–308.
[35] E.B. Park, K.J. Kim, H.R. Jeong, J.K. Lee, H.J. Kim, H.H. Lee, J.W. Lim, J.S. Shin, A. Koeberle, O. Werz, K.T. Lee, J.Y. Lee, Synthesis, structural determination, and biological evaluation of phenylsulfonyl hydrazide derivatives as potential anti-inflammatory agents, Bioorg. Med. Chem. Lett. 26 (2016) 5193–5197.
[36] D. Das Mukherjee, N.M. Kumar, M.P. Tantak, A. Das, A. Ganguli, S. Datta, D. Kumar, G. Chakrabarti, Development of novel Bis(indolyl)-hydrazide-hydrazone derivatives as potent microtubule-targeting cytotoxic agents against A549 lung cancer cells, Biochemistry 55 (2016) 3020–3035.
[37] W. Gu, X.Y. Jin, D.D. Li, S.F. Wang, X.B. Tao, H. Chen, Design, synthesis and *in vitro* anticancer activity of novel quinoline and oxadiazole derivatives of ursolic acid, Bioorg. Med. Chem. Lett. 27 (2017) 4128–4132.
[38] X.Y. Jin, H. Chen, X.B. Tao, S.F. Wang, W. Gu, Synthesis and antitumor activity of novel quinoline derivatives of ursolic acid, J. Forestry Eng. 3 (2018) 54–64.
[39] M.L. Circu, T.Y. Aw, Reactive oxygen species, cellular redox systems, and apoptosis, Free Radical Bio. Med. 48 (2010) 749–762.
[40] A.T. Dharmaraja, Role of reactive oxygen species (ROS) in therapeutics and drug resistance in cancer and bacteria, J. Med. Chem. 60 (2017) 3221–3240.
[41] Z. Song, C.P. Chen, J. Liu, X.A. Wen, H.B. Sun, H.L. Yuan, Design, synthesis, and biological evaluation of (2*E*)-(2-oxo-1,2-dihydro-3H-indol-3-ylidene)acetate derivatives as anti-proliferative agents through ROS-induced cell apoptosis, Eur. J. Med. Chem. 124 (2016) 809–819.
[42] J.N. Chen, X.F. Wang, T. Li, D.W. Wu, X.B. Fu, G.J. Zhang, X.C. Shen, H.S. Wang, Design, synthesis, and biological evaluation of novel quinazolinyl-diaryl urea derivatives as potential anticancer agents, Eur. J. Med. Chem. 107 (2016) 12–25.
[43] E. Finkel, The mitochondrion: Is it central to apoptosis? Science 292 (2001) 624–626.
[44] S. Gupta, G.E.N. Kass, E. Szegezdi, B. Joseph, The mitochondrial death pathway: a promising therapeutic target in diseases, J. Cell Mol. Med. 13 (2009) 1004–1033.
[45] N. Parikh, C. Koshy, V. Dhayabaran, L.R. Perumalsamy, R. Sowdhamini, A. Sarin, The N-terminus and alpha-5, alpha-6 helices of the pro-apoptotic protein Bax, modulate functional interactions with the anti-apoptotic protein Bcl-xL, BMC Cell Biol. 8 (2007) 16.
[46] S.T. Xu, H. Yao, S.S. Luo, Y.K. Zhang, D.H. Yang, D.H. Li, G.Y. Wang, M. Hu, Y. Y. Qiu, X.M. Wu, H.Q. Yao, W.J. Xie, Z.S. Chen, J.Y. Xu, A novel potent anticancer compound optimized from a natural oridonin scaffold induces apoptosis and cell cycle arrest through the mitochondrial pathway, J. Med. Chem. 60 (2017) 1449–1468.
[47] S. Li, X.Y. Li, T.J. Zhang, M.O. Kamara, J.W. Liang, J. Zhu, F.H. Meng, A novel potent anticancer compound optimized from a natural oridonin scaffold induces apoptosis and cell cycle arrest through the mitochondrial pathway, Bioorg. Chem. 94 (2020), 103385.
[48] A.H. Boulares, A.G. Yakovlev, V. Ivanova, B.A. Stoica, G. Wang, S. Iyer, M. Smulson, Role of Poly(ADP-ribose) Polymerase (PARP) cleavage in apoptosis. Caspase 3-resistant PARP mutant increases rates of apoptosis in transfected cells, J. Biol. Chem. 274 (1999) 22932–22940.
[49] G. Hoxhaj, B.D. Manning, The PI3K–AKT network at the interface of oncogenic signalling and cancer metabolism, Nat. Rev. Cancer. 20 (2020) 74–88.
[50] S.S. Wang, Q.L. Zhang, P. Chu, L.Q. Kong, G.Z. Li, Y.Q. Li, L. Yang, W.J. Zhao, X. H. Guo, Z.Y. Tang, Synthesis and antitumor activity of α, β-unsaturated carbonyl moietycontaining oleanolic acid derivatives targeting PI3K/AKT/mTOR signaling pathway, Bioorg. Chem. 101 (2020), 104036.
[51] H.X. Zhang, Y. Kang, N. Li, H.F. Wang, Y.R. Bao, Y.W. Li, X.Z. Li, Z. Jiang, G. Chen, Triterpenoids from *Liquidambar Fructus* induced cell apoptosis via a PI3K-AKT related signal pathway in SMMC7721 cancer cells, Phytochemistry 171 (2020), 112228.
[52] K.C. Lee, Y.L. Chen, P.Y. Lin, W.L. Chuang, Ursolic acid-induced apoptosis via regulation of the PI3K/Akt and MAPK signaling pathways in Huh-7 cells, Molecules 23 (2018) 2016.
[53] H. Yun, D.W. Hua, T.T. Miao, S.F. Wang, X.Y. Jin, W. Gu, Synthesis, crystal structure and antitumor activity of a new indolequinone derivative of ursolic acid, Chinese J. Struct. Chem. 35 (2016) 1167–1173.
[54] Y.P. Song, Z.Y. Xin, Y.M. Wan, J.B. Li, B.P. Ye, X.W. Xue, Synthesis and anticancer activity of some novel indolo[3,2-b] and rographolide derivatives as apoptosis-inducing agents, Eur. J. Med. Chem. 90 (2015) 695–706.
[55] C.C. Su, J.Y.F. Chen, Z.H. Din, J.H. Su, Z.Y. Yang, Y.J. Chen, R.Y.L. Wang, Y.J. Wu, 13-acetoxysarcocrassolide induces apoptosis on human gastric carcinoma cells through mitochondria-related apoptotic pathways: p38/JNK activation and PI3K/AKT suppression, Mar. Drugs 12 (2014) 5295–5315.
[56] Y.C. Li, Z.Y. Gu, C. Zhang, S.H. Li, L. Zhang, G.Q. Zhou, S.X. Wang, J.C. Zhang, Synthesis, characterization and ROS-mediated antitumor effects of palladium(II) complexes of curcuminoids, Eur. J. Med. Chem. 144 (2018) 662–671.